

# ElutoCAT Drug-Eluting Thoracic Catheter

Emily Blick, Christopher Hiner, Katherine Jones, Drishti Maniar, and Thea Ornstein  
Clinical Advisor: Dr. Joseph S. Friedberg, Division of Thoracic Surgery Head, University of Maryland School of Medicine  
Research Advisor : Associate Professor Christopher Jewell, Department of Bioengineering, University of Maryland



## Introduction

Thoracic catheters, also known as a chest tube, is inserted into the pleural cavity and helps with the drainage of fluid, blood and air from the plural space.



Figure 1. Medical procedure for chest tube insertion [1].

**Problem:** the insertion and continuous presence of the tube for 1-2 weeks causes patient pain that cannot be solved with current treatments such as local analgesic injections, epidural and intravenous analgesic. Patient's Chronic pain influences the physician's ability to repeatedly remove and reinsert the tube and respiratory splinting. Physicians and our main motivator is enhancing **patient comfort**.

*"Thoracic catheters have NOT CHANGED in the past 25 years...patients complain of chest tube discomfort MORE THAN any other aspect of the surgical procedure."* — Dr. Joseph Friedberg

## Our Solution: ElutoCAT

- Proposed Solution:** a analgesic-eluting, silicon thoracic catheter that releases lidocaine from a polymer coating to mitigate patient pain

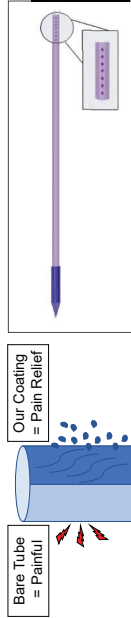


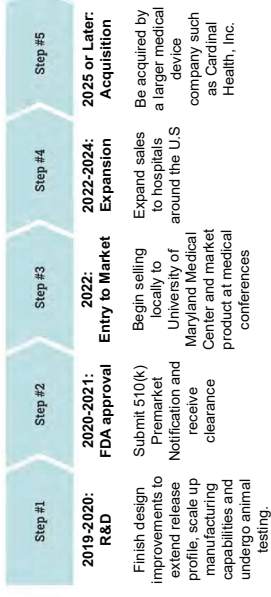
Figure 2. Comparison between desired effects of old and new product.

Figure 3. CAD drawing of ElutoCAT.

- Long-Term Value:** mitigation of patient pain in a cost-effective manner

## Business Plan

- Current thoracic catheters generate ~\$20 of revenue per unit. ElutoCAT is planned to sell for \$50 per unit.
  - Increased price is feasible due to time and cost saved by hospital.
  - Marketing will target hospitals and, more specifically, their surgeons as customers for the product.
- Total Global Market Revenue in 2016: **\$280 M** [2]
- Compound Annual Growth Rate of **6.5%**
- Predicted Global Market Revenue in 2024: **\$410 M** [3]
- The ultimate goal of the ElutoCAT is to phase out conventional thoracic catheters around the world**



## Methods: Solvent Selection

- Purpose:** To select the appropriate polymer-solvent combination.
- Methods:** Each polymer was placed in each solvent and observed for complete dissolution after 15 minutes and after 3 days of shaking. The polymers tested were polycaprolactone (PCL), 50:50 poly(lactic-co-glycolic acid) (PLGA) and polyethylene glycol (PEG). Triplicates were completed. Protocol is described in Figure 4.
- Results:** DCM was shown to dissolve all polymers after 15 minutes. PLGA was shown to dissolve in acetone. All other solvents failed to dissolve the polymers. The same results were seen after both time periods.
- Takeaway:** PLGA was chosen as our polymer and DCM as our solvent.

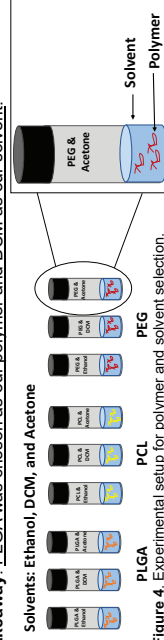


Figure 4. Experimental setup for polymer and solvent selection.

## Prototyping: Dip Coating

- Purpose:** To coat the silicon tube with 600mg/ml of lidocaine and 100mg/ml of PLGA.
- Methods:** 10 mm x 2 mm slabs of silicon were either 1) uncoated, 2) coated with 600mg/ml of lidocaine, 3) coated with 100mg/ml of PLGA or 4) coated with a mixture of 600 mg/ml lidocaine and 100mg/ml of PLGA. UV spectroscopy and scanning electron microscopy (SEM) was performed. Triplicates were completed. Protocol is described in Figure 5.
- Results:** Spectroscopy showed that on average 1.5 mg of lidocaine was loaded per 100 mm<sup>2</sup> of tube (Figure 6). SEM images showed PLGA-lidocaine on the cross section of a silicon tube (Figure 7). The resulting scan of PLGA and lidocaine had a peak at 263 nm, confirming the presence of lidocaine in the coating (Figure 8).
- Takeaway:** PLGA-lidocaine mixture was coated on the silicon tube.

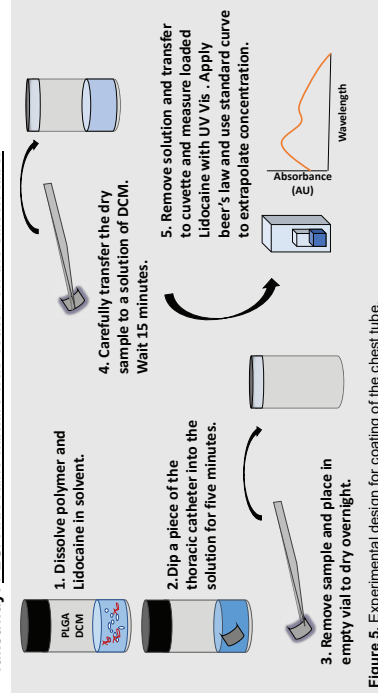


Figure 5. Experimental design for coating of the chest tube.

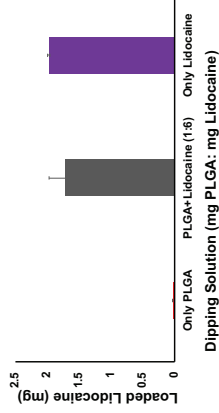


Figure 6. Mass of lidocaine coated onto silicon tube fragments, coated with PLGA and lidocaine (100 mg/ml: 600 mg/ml), only PLGA and only lidocaine. From the PLGA+ lidocaine coating, 1.5 mg of lidocaine on average was loaded per 100 mm<sup>2</sup> of tube.

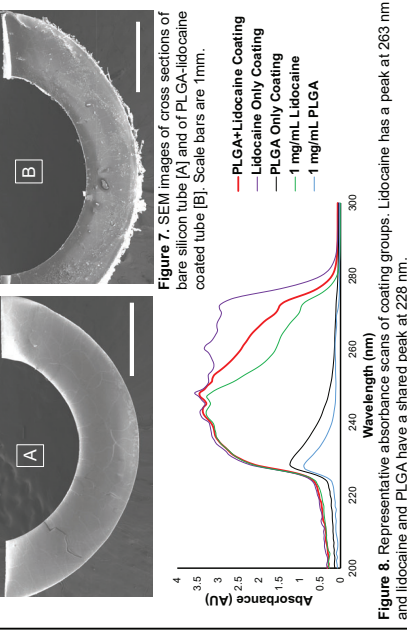


Figure 7. SEM images of cross sections of bare silicon tube [A] and of PLGA-lidocaine coated tube [B]. Scale bars are 1mm.

## Testing: Elution Study

- Purpose:** To elute lidocaine from coated silicon tube.
- Methods:** PLGA-lidocaine coated silicon tubes were made as described in Figure 5. Tubes were immersed in a phosphate buffer for 1 hour and UV spectroscopy was performed on the solution every 5-10 minutes. Triplicates were completed.
- Results:** All loaded lidocaine (0.75 mg/ 100 mm<sup>2</sup> of tube) was eluted over 20 minutes (Figure 9).
- Takeaway:** Lidocaine can elute out of the PLGA coating in a time dependent manner.

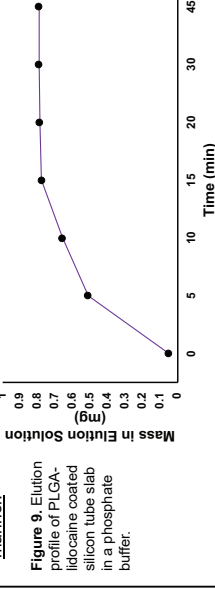


Figure 9. Elution profile of PLGA-lidocaine coated silicon tube slab in a phosphate buffer.

## Conclusions and Future Work

- Demonstrated that thoracic catheters can be coated with a polymer and analgesic together.
- Exhibited that lidocaine can be released from a chest tube over a short period of time.
- Established that lidocaine elution from thoracic catheters has promise for being a viable pain management technique.
- Future goals include increasing duration of sustained release, further characterizing coating with mechanical testing and devising protocols to scale-up production for entire chest tubes. In terms of **ethical implications**, animal and clinical trials will be completed to demonstrate safety and efficacy. No data can be fabricated to make the device appear any more safe or effective than it actually is.

## References

- Heller, Jacob. (2016). Chest tube insertion. Retrieved from [https://medlineplus.gov/ency/presentations/100008\\_4.htm](https://medlineplus.gov/ency/presentations/100008_4.htm)
- Global Chest Drainage Catheters Market Report 2017. (2017). Retrieved from <https://www.slideshare.net/finvagu11/global-chest-drainage-catheters-market-research-report-2017>
- MarketWatch. (2016). At 6.5% CAGR... Retrieved from <https://www.marketwatch.com/press-release/at-65-cagr-thoracic-catheters-market-size-set-to-register>

## **ElutoCAT Drug-Eluting Thoracic Catheter**

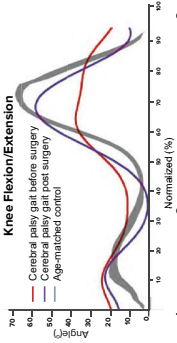
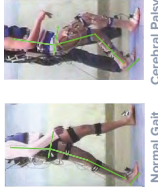
Emily Blick, Christopher Hiner, Katherine Jones, Drishti Maniar, & Thea Ornstein

Thoracic surgery is an operative process that focuses on chest organs such as the heart, lungs, esophagus and the trachea. The surgery results in significant postoperative and chronic pain which is mainly caused by the insertion and continuous placement of a thoracic catheter in the patient's pleural space for up to 2 weeks. The insertion of the thoracic catheter, or better known as the chest tube, is imperative to drain air, fluid and blood post-operation. Current pain management strategies such as local analgesic injections, thoracic epidural or intravenous painkillers, fail to deliver localized, sustained pain relief to patients for the entirety of the time period in which they have a chest tube placement. Thus, we aimed to provide long-term patient pain relief by designing a silicon, drug-eluting thoracic catheter which would slowly elute lidocaine at the site of chest tube insertion, over a one week period. To demonstrate proof of concept, small slabs of silicon catheter were experimented on. The optimal dissolvable polymer, solvent and polymer to lidocaine ratios were determined via the dip-coating method. By performing UV spectroscopy and scanning electron microscopy, we demonstrated that we effectively coated a portion of a silicon chest tube in a polymer-lidocaine mixture and successfully eluted lidocaine from the coated tube into phosphate buffer saline over an hour. Future work will focus on increasing the amount of lidocaine loaded in order to reach physiologically relevant levels as well as key manufacturing processes that will enable product scale-up.

# Knee Extension Monitoring Device For Children with Cerebral Palsy

Group Two: Viswanath Gorti, Zain Kaz, Nikita Kedtia, Mateo Reveiz, Janette Yacynych  
 Advisors: Dr. White, Department of Bioengineering, University of Maryland and Dr. Pergami, Children's National

## Motivation



**Cerebral Palsy** is the most frequent cause of motor disability in children and causes complex & heterogeneous **gait deviations**.

## Objective

**Existing treatment** methods include frequent physical therapist sessions that are **time consuming** and **expensive**.

We aim to develop an **at-home** and **affordable** gait monitoring system that enables patients to make **significant improvements** and thus increase their **independence** and **quality of life**.

## Ethical Considerations



Child safety



Physician-patient relationship



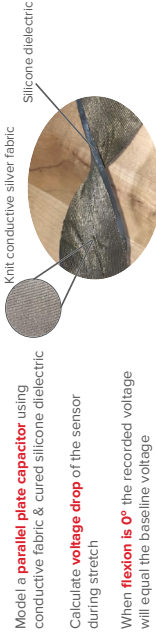
Comfort of device



Affordable to all patients

## Methods and Results

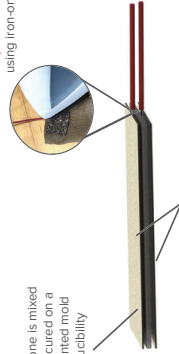
### Approach A: Stretch Strain Sensor



### Fabrication

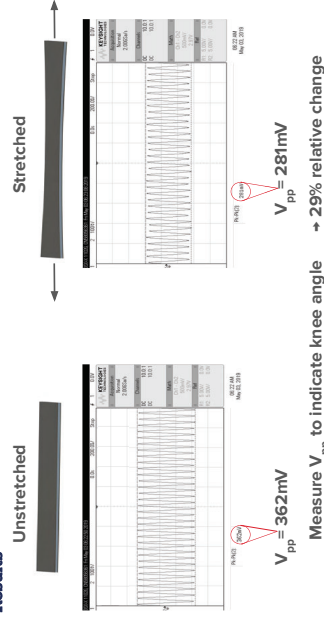
**Step 2:** Ecoflex® silicone is mixed 1A:1B by weight and cured on a hot plate in a 3D printed mold made for reproducibility

**Step 1:** Attach wires using iron-on decal

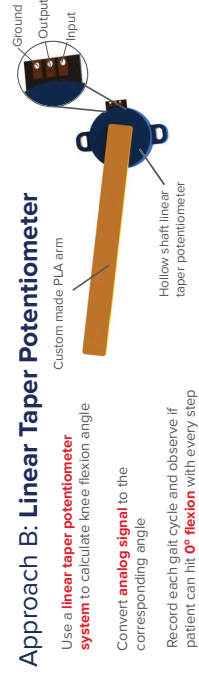


**Step 3:** Use thin layer of uncured silicone to attach the conductive fabric on each side of the rubber silicone. Cut sensor to size.

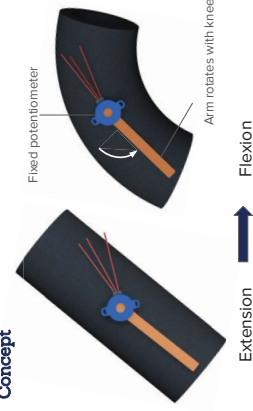
### Results



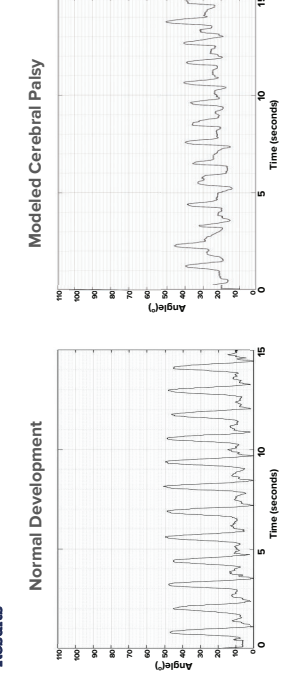
## Software and Electronics



### Concept

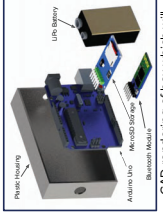
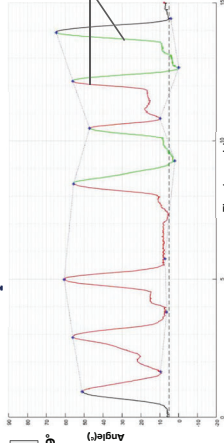


### Results



### Graphical User Interface

**START**  
 Average max: 55.9°  
 Average min: 5.7°  
 Cycles performed correctly: 33.3%



CAD rendering of box which will house all electrical components

Circuit diagram of the strain sensor design.

Circuit diagram of the potentiometer design.

## Conclusion and Future Work

### Conclusion

The **potentiometer system** provides a more **precise** knee flexion angle measurement and enables real-time **feedback** and **classification** of gait cycles

### Future Work

**Sleeker design** to improve comfort of device

Pair device with **step sensor** for a more detailed analysis of gait

**Adjustability** for wider age range and broader applications

## **Knee Extension Monitoring Device for Children with Cerebral Palsy**

Viswanath Gorti, Zain Kazi, Nikita Kedia, Mateo Reveiz, Janette Yacynych

Cerebral palsy (CP) is a neurological disorder which impairs movement, muscle tone, and posture. Clinical studies have found differences associated with knee angles in children with CP relative to healthy children that result in difficulty walking. Unlike healthy children, children with CP are unable to extend their knees to a full  $180^\circ$  when walking, resulting in a crouched gait pattern. These patients must be monitored by clinicians, including physical therapists, to ensure proper knee extension. This treatment can be time consuming and expensive. According to the Center for Disease Control and Prevention, the lifetime cost for a person with CP is 1.175 billion dollars, including physician visits, assistive devices, therapies, rehabilitation, and other long term-care options. The average copay for a weekly physical therapist appointment is \$30 and patients with CP would need constant monitoring of this movement, which would accrue additional costs. Existing knee angle monitoring devices on the market are expensive and not tailored for pediatric patients. Here we present a low-cost device that will allow patients to receive at-home, direct feedback based on the knee angle measurements. The patient will be notified with the percentage of steps he or she took correctly and the gait cycles will be automatically detected and classified via a software application. This recorded data can also be stored and sent to the physician for daily tracking of the patient's progress. Two approaches were compared for measuring knee angles: a stretchable strain sensor that modeled a parallel plate capacitor and resulted in a voltage drop with stretch, and a linear taper potentiometer in which the analog signal was converted to the corresponding angle. After testing both sensors, it was determined that the potentiometer system provided more precise and reliable angle measurements. Knee angle measurements for healthy gait and crouched gait were recorded and compared. In the future, we will pair our device with a step sensor to allow for a more detailed analysis of the patient's gait. We plan on testing our device clinically and this testing will be validated against the current physical therapy treatment.

# Minimally Invasive Glucose Sensing Device

Medina Alogba, Kyran Gibson, Mike Mistretta, Alex Paskal, Cynthia Uzoukwu

Advisor(s): Dr. Edward Eisenstein, Fischell Department of Bioengineering, University of Maryland, Dr. Johana Diaz, University of Maryland School of Medicine

## Motivation

It is estimated that ~15 million babies are born preterm. Preterm birth complications are the leading cause of death in children under the age of 5. There are degrees of severity of preterm birth depending on the amount of gestation, which ranges from extremely preterm: < 28 weeks, very preterm: 28-32 weeks, and moderate to late preterm: 32-37 weeks

Series of tests are performed on infants in the NICU to varying degrees which depend on the severity of their preterm birth. One tests performed consistently on infants in the NICU is the **blood glucose test**, blood is obtained from the infants via heel pricks or arterial lines in order to measure their glucose level.

Neonates are faced with potential issues such as **anemia due to immense drawing of blood** and **abnormal gait when the infants begin to walk** as a result of the pain from heel pricking. Heel pricks have been observed to cause swelling, redness, neonatal staphylococcal, and inguinal adenitis.



## Objective

The project goal is to create a minimally-invasive medical device that can be used to measure blood glucose concentration using interstitial fluid. This device is a necessity in the neonatal intensive care unit (NICU) as the device will be able to:

- **Decrease amount of blood drawn** from neonates to reduce instances of anemia
- **Reduce use of heel pricking** to decrease amounts of infection and possible abnormal gait when the infants begin walking

Additionally we hope that future work can help to reduce the amount of leads that are placed on neonates which can cause discomfort for both neonates and nurses.

## Methods

### Concept Design



### Proof of Concept

- Hollow microneedles have been empirically demonstrated to be collecting a sufficient quantity (>2µL) of interstitial fluid for glucose strip saturation over a clinically acceptable period (<30s)

### Prototype Design

- **SolidWorks** was used to create the sampling component and microneedle patch
- The prototype was printed using **PLA** material on the **FDM 3D printing machine**
- Microneedle patch to be 3D-printed using **NanoScribe 3D printer**

### Prototype Testing

- Powdered glucose was incubated in 8 varying concentrations of 2 mmol to 20 mmol for a period of 2 weeks prior to testing
- Glucose strips were saturated with the various concentrations and **Rodeostat potentiostat** was used to apply a voltage to the electrodes on the glucose strips to induce current
- Triplicate measurements of current vs. time were collected for each glucose concentration
- Current at time t=4s was extrapolated for each glucose concentration, to create a **look-up table for calibration** of the analytical component of the device

## Results

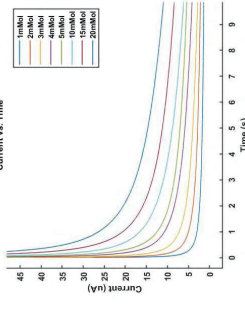
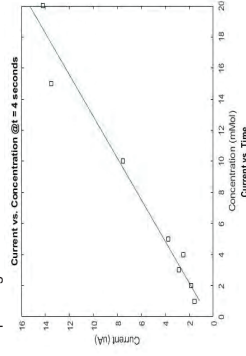
### Sampling Component

- Sampling component FEA proved difficult in SolidWorks
- Material would be changed to an FDA approved medical device material



### Analytical Component

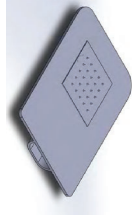
A linear regression was performed at time t = 4 to estimate a function relating current and concentration. This linear relationship allows us to estimate the concentration of glucose corresponding to a measured current.



### Microneedle

- Difficulties in printing abilities of Terrapin Works
- FEA of CAD was used to prove the feasibility of the patch
- Future work consists of new printing strategy

### Finished Prototype Design



## Ethical Implications

Neonatal safety and comfort were of top priority when designing the sampling component and microneedle patch. During the design process, these ethical criteria were considered:

- Material constraints to minimize any possible negative impacts on the neonate's health or comfort
- Materials considered are biocompatible or biocompatible
- Whether nurses and doctors would be positively affected by our device by being able to conduct tests in a timely manner
- Parents would be able to watch their baby undergo a less invasive method of testing
- No person (neonate, nurse, doctor) could undergo any significant risk from our device

## Future Work & Conclusion

### Microneedle

- The microneedle patch ideally will be 3D printed for performance efficiency using the polymer **PEEK** due to its chemical inertness and biocompatibility. However, constraints such as price, printability and manufacturing time may require us to make use of other materials such as PLA, PLGA, or silicon
- Remaining design criteria and constraints will be considered to **optimize flow through the microneedles**

### Collection Component

- To prevent any form of accident that may occur, we are suggesting that the sampling component, should be printed using the **M6000 printer Stratasys Object 500 with a printing material Connex3**
- A biocompatible adhesive, **Cyberbond 5000**, will be used to adhere the microneedle patch to the sampling component. This adhesive is commonly used for medical devices and is provided by the company H.B. Fuller
- Experiments determining collection capacity will be performed

### Point-of-Care

The major impact this device can lead to is its potential to be used to **analyze other analytes found in interstitial fluid**. Its application can be a foundation to create a **point-of-care glucose measuring device** in not only neonates but children ranging two years old and younger as it may be used to diagnose hyperglycemia and hypoglycemia similar to an adult glucose meter.

### Conclusion

Glucose concentrations within the clinically relevant range (5-10 mmol) can be measured accurately and reliably using chronoamperometric methods in conjunction with standard glucose strips saturated with glucose water. Provided hollow microneedles can be reliably and affordably manufactured and can produce sufficient volume of ISF, the ease of fabrication and convenience of our device makes it an excellent alternative to existing minimally-invasive and non-invasive glucose monitoring devices.

## References

1. Katzer, A., Marquardt, H., Westendorf, J., Wienting, J., & Von Foerster, G. (2002). Polyetheretherketone— cytotoxicity and mutagenicity in vitro. *Biomaterials*, 23(8), 1749-1759. doi:10.1016/S0142-9612(01)00300-0
2. Kurtz, S. M., & Davies, J. N. (2007). PEEK biomaterials in trauma, orthopaedic, and spinal implants. *Biomaterials*, 28(92), 4945-4969. doi:10.1016/j.biomaterials.2007.07.013
3. Waghule, T., Singhi, G., & Dubey, S. (2018, November 09). Microneedles: A smart approach and increasing potential for transdermal drug delivery system. Retrieved from <https://www.sciencedirect.com/science/article/pii/S0753332118345091>
4. Wenz, L., Merritt, K., Brown, S., Moeet, A., & Steffes, A. (1980). In vitro biocompatibility of polyetheretherketone and polysulfone composites. *Journal of Biomedical Materials Research*, 24(2), 207-215.

## **Minimally Invasive Glucose Sensing Device**

Medina Alogba, Kyran Gibson, Mike Mistretta, Alex Paskal, Cynthia Uzoukwa

According to the World Health Organization, an estimated 15 billion infants are born preterm every year. Preterm birth complications are the leading cause of death of children under the age of 5. Infants are considered preterm when born earlier than thirty-seven weeks. These infants are at a high risk of severe health complications requiring them to be constantly monitored. Premature infants are kept in isolettes that control their environment where they are connected to a multitude of machines that monitor their vitals constantly. Continuous health monitoring allows nurses and doctors to determine the best treatment each infant needs to facilitate growth. One of the most common blood tests is the blood glucose test. Blood for this test is collected via a heel prick, an arterial line, or venepuncture. Glucose testing needs to be performed multiple times throughout the day leading to a large cumulative sample of blood taken from the neonates. We have developed a two-component medical device that can measure interstitial fluid glucose levels that are able to be related to blood glucose levels. The first component is a sampling device that uses microneedles to collect the neonate's interstitial fluid. The second component is an analytical component that will analyze the interstitial fluid for glucose measurements. Our instrument would provide doctors with a reliable, minimally-invasive method for measuring interstitial glucose concentration, thus mitigating the need to repeatedly draw blood from the infants and reducing the amount of risk at which they are exposed.

# A Laparoscopic Tool for Pediatric Epicardial Lead Removal

Alex Wahi, Manav Parikh, Amelia Hurley-Novanty, Lauren Fowlkes, Shaanit Sen

Advisors: Professor Dr. Hubert Montas, Department of Bioengineering, University of Maryland, Dr. Rohan Kumthekar, Children's National Hospital

## Background

### Problem

- Pacemaker placed in abdominal rather than chest cavity of pediatric patients
- Once pacemaker is removed, epicardial leads are abandoned on heart
- Only current lead removal option is open heart surgery
- Patients with abandoned leads have a decreased quality of life

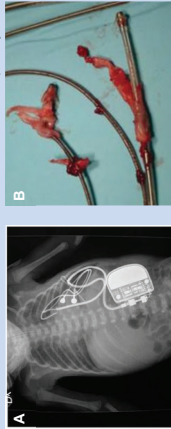


Figure 1. Epicardial leads abandoned in children. A) X-Ray image of abdominal pacemaker. Arrows point to attachment site of epicardial leads onto the heart. B) Fibrotic adhesions on removed epicardial leads from porcine model.

### Objective

Design a novel epicardial lead removal device, with 5 degrees of freedom for use in a pediatric population which is compatible with the port designed by Dr. Rohan Kumthekar and his engineering team at Children's National Hospital.

## Design Requirements

### Design Overview

- Designed for precise movements
- Designed to have 5 degrees of freedom
- Simple user inputs
- Compatible with port
- Ease of use for surgeon



## Cutting Methods

Criteria	Cutting Options		
	Laser	Electrocautery	Harmonic Scalpel
Efficiency	4	4	3
Cost	1	4	2
Risks	2	3	3
Total	7	11	8

## Electrocautery Benefits:

- Non-directional cutting
- 100-1200 temperature range
- Minimum risks

## Prototype Design

### Articulating Tip

- Designed for precise movements (5 mm radius of curvature)
- A single flexible piece contracted using an articulation cable

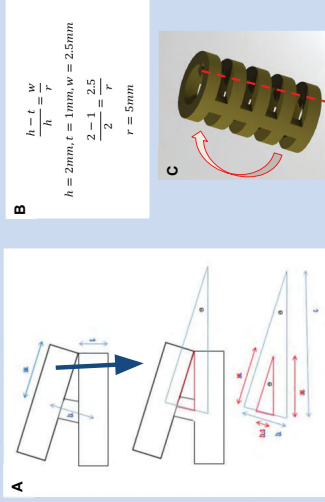


Figure 2. Tip of the device articulates by shortening a cable, which contracts the flexible piece on the end. A) Derivation of calculations for radius of curvature. B) Calculations of radius of curvature. C) Rendered CAD image of articulating tip. Pulling on the cable (represented by dotted arrow) causes the tip to curve towards that side.

### Handle Input to Tip

- Movement of the proximal handle pulls the articulation cable and contracts the articulating tip



Figure 3. Handle design for movement of articulation cable. A) CAD image of assembled handle. Upon movement of the diagonal piece about the fulcrum, the cable is pulled, resulting in contraction of the tip. Solid line represents cable, dotted line represents arm of action. B) Exploded view of assembled handle.

### Handle Input for Rotation

- Rotation based on the movement of two gears, one exposed and one hidden inside shell of handle
- Rotation of exposed gear with index finger leads to the rotation of the outer shell



Figure 4. Gear mechanism for rotation of the device.

## Discussion

### Ethical Implications

- Allows for removal of leads in children, which improves quality of life by allowing child to undergo MRI scans and alleviating risk of infection of abandoned leads
- Reduces strain put on the surgeon during traditional laparoscopic surgery by increasing ergonomics and range of motion
- Promotes less invasive procedures for other surgeries

### Regulatory Pathway

- Will need to file for IACUC approval for animal testing in pig model
- Will need to file for IRB approval for testing in operating rooms
- Class II Device - requires 510K
- Receive Independent Device Exemption (IDE) for clinical trials

### Market Potential

- Immediate market of those in need of epicardial lead removal
- Sell the tool as an one use laparoscopic medical device to hospitals
- Market will expand with the growth of laparoscopic procedures

## Future Work

Formal in vivo testing in animals models

Begin clinical trials once IDE is acquired

Explore other applications of tip such as removal of ovarian cysts or other growths safely accessed through laparoscopy where precision is required to avoid damaging important surrounding tissue

Incorporation of other functionality at tip (for example, graspers)

## References

1. Posthumus, G. A. J. Retrieved December 17, 2018, from <https://www.ncbi.nlm.nih.gov/pubmed/29222428>
2. Gillis, A. M. (2017, January 16). Lead Abatement of Lead. Retrieved December 17, 2018, from <http://www.leadabatement.com/resources/lead-abatement-101/>
3. Living with a pacemaker (n.d.). Retrieved October 8, 2018, from <http://www.nhs.uk/conditions/living-with-a-pacemaker/>
4. Current Lead Classification and Correlation with Harverson Lead Extraction Results. Retrieved December 17, 2018, from <https://www.ncbi.nlm.nih.gov/pubmed/30222428>

## **A Pediatric Laparoscopic Tool for Epicardial Lead Removal**

Alex Wahl, Manav Parikh, Amelia Hurley-Novanty, Lauren Fowlkes, Shaanit Sen

Infants with severe cardiac problems may require implantation of a pacemaker into the abdomen with a lead which is attached to the epicardial surface. These pacemakers only last up to 10 years, and eventually must be replaced with a transvenous lead. During this procedure, the epicardial lead, which lies in the abdominal and thoracic cavities, is abandoned except in emergency situations. Given that these leads have adhesions to vital organs and directly to the heart, removal requires open heart surgery. Leaving this lead results in decreased quality of life for these patients since they can no longer undergo magnetic resonance imaging procedures or go through metal detectors without issue. Current laparoscopic devices, which would make the procedure less invasive, are not appropriately sized for a pediatric population. Additionally, many tools are difficult to use and require many manual inputs to achieve relatively little mobility. We have designed and prototyped a laparoscopic device with five degrees of freedom and higher precision than current models, in order to remove adhesions in the size scale found in pediatric patients. This device couples existing electrocautery components with a novel articulation mechanism, which includes an articulating tip directed by mechanical surgeon inputs. The articulation mechanism within the body has a small,  $<1$  cm bending radius to maneuver around small adhesions and organs for patient safety and efficacy during surgery. The direction of the electrocautery wire will be controlled by this articulation mechanism. This modality will allow adhesions to be easily cut, is widely used in the operating room, and reduces the risk of patient bleeding. It is also physician-controlled to prevent damage to any surrounding tissue. This tool will be utilized with a laparoscopic camera, insufflation, and a pediatric port designed at Children's National Hospital. The system of these tools is expected to allow removal of adhesive epicardial leads in pediatric patients, increase the safety of the removal procedure, and improve the overall quality of life for these patients. Beyond this immediate intended use, this tool may also be used in other pediatric surgeries, which could lead to better surgical outcomes from less invasive procedures.



# High-Flux Hemofiltration System for Rapid Toxin Removal

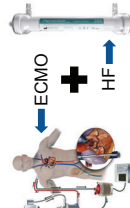
Morgan Hoffman, Daniel Hopkins, Morgan Janes, Milan Patel, and Manaaail Rao  
 Advisors: Dr. Helim Aranda-Espinoza<sup>1</sup>, Dr. Allison Grazioli<sup>2</sup>, Dr. Zhongjun Wu<sup>2</sup>, Dr. Josh King<sup>2</sup>  
<sup>1</sup>Fischell Department of Bioengineering, University of Maryland <sup>2</sup>University of Maryland School of Medicine

## Background and Objectives

Acute poisonings affect 2.16 million people each year.<sup>1</sup> Unfortunately, traditional removal modalities such as hemofiltration (HF) typically are not useful for toxins that have a high protein binding fraction or volume of distribution. These toxins are termed non-dialyzable (ND), and overdoses frequently result in death.

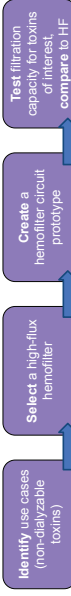
Toxin	Purpose	Protein Bound	Dialyzable?
Codichone	Anti-inflammatory	40-50%	No
Flecainide	Anti-arrhythmic	40%	No
Metformin	Anti-diabetic	Negligible	Yes

Left: Hemofiltration process with a single filter.  
 Above: Candidate non-dialyzable and dialyzable toxins.  
 Below: High flow design concept combining ECMO flow rate with HF removal modality.<sup>2</sup>



Conventional HF methods are inadequate for ND toxins due to low blood flow rates and an insufficient membrane surface area. Extracorporeal membrane oxygenation (ECMO) is a technology for heart and lung failure that circulates blood at 4-5 L/min.

**Objective:** Develop an **ECMO-compatible hemofiltration system** with an increased surface area to facilitate **rapid acute toxin removal** at high flow rates for the treatment of poisoning victims.



## Design Specifications

**System Design**

- Parallel flow circuit
- 8 filters
- 4 L/min total flow
- 500 mL/min per filter

HF removal: 41 mg/hour

Our design: 1,000 mg/hour

System ultrafiltration: 2.437 mL/min

Filter ultrafiltration: 305 mL/min

**Filter Selection**

Parameter	Revaclear 300
Blood flow rate > 400 mL/min	500 mL/min
TMP allowance > 400 mm Hg	600 mm Hg
High ultrafiltration coefficient	48 mL/hr*mm Hg
Cost < \$800	\$219.95 for 24
Middle molecule removal	Yes, 70% β2M



300  
Baxter Revaclear  
Capillary Dialyzer<sup>3</sup>

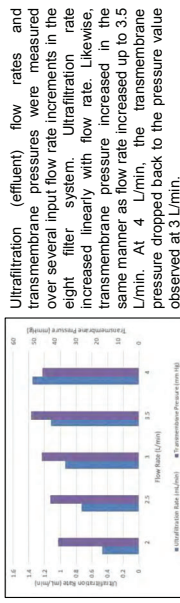
## Methods

**Parallel Eight Filter System** - Seven Y connectors were used on each of the inlet, outlet, and effluent ends of the eight filter group to produce one system inlet, outlet, and effluent tube. The inlet tube is attached to the ECMO pump, while the outlet tube connects to the replacement bag. The effluent tubing is placed into an empty bucket to discard the ultrafiltrate.

**Pressure and Flow Sensors** - Flowmetric sensors were attached to the main input, output, and effluent tubing to monitor flow rates. Pressure sensors were attached at the same locations on an individual filter in the system to measure the transmembrane pressure (TMP).

**Toxin** - Flecainide was used to test the performance of the system because it is non-dialyzable. The initial concentration was the plasma concentration for a 5,000 mg overdose in an 80 kg adult (6.8 µg/mL). Flecainide was dissolved in 5 L of saline. Samples were taken from the effluent outflow and the concentration of flecainide was measured with UV-visible spectroscopy.

## Results



Eight filters  
 Effluent flow rates (L/min)  
 Measured 1.87  
 Target: 2.44

Flecainide concentration over time is shown in a two filter system with flow rate 1 L/min (above left), and in an eight filter system with flow rate 4 L/min (above right). Mass removal rates over time were then calculated in mg/hr (below). Potential removal rate represents the theoretical rate given addition of an effluent pump to reach the target ultrafiltration rates. The possibility of moderate flecainide adsorption onto the hemofilters may contribute partially to the observed decrease in concentration.

Filter Number	Average removal rate	Initial removal rate	Potential removal rate	Target removal rate	Percent error
2	52.9	115.0	175.0	250	30%
8	178.9	684.4	891.9	1000	10.81%

2.16M Poison Exposure Cases  
 0.0004% require ECMO\*

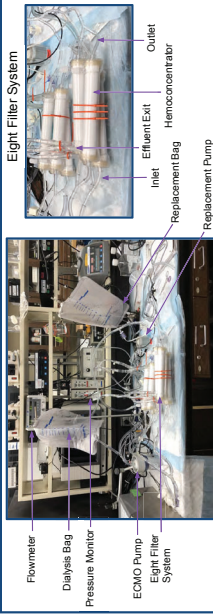
PT  
 891.9 mg/hr

CWH  
 41 mg/hr

Filtering capacity x 21.6

Annual \$63M  
 697 per Patient

## Prototype



## Ethical Implications

While some poisoning patients may already require ECMO for heart and/or lung failure, others may not. For these patients, the risks of ECMO including bleeding, clotting, hemolysis, and air embolism<sup>5</sup> must be outweighed by the benefits. Our modality also requires rapid addition of replacement fluid to the blood, which can lead to hemodynamic instability. However, the ECMO system is designed to mitigate this general complication. Regardless, providers must use their best acute judgment to determine whether or not our system will be safe for each individual patient.

## Conclusions and Future Work

Developed a **parallel hemofilter system** that:

- Supports an ECMO-compatible flow rate of 4 L/min
- Removes the toxin flecainide at a clinically relevant rate of 684.4 mg/hr, with a potential rate of 891.9 mg/hr with an effluent pump
  - Demonstrates a potential 21.6-fold increase in removal rate compared to conventional hemofiltration

**Clinical contribution:** A robust, time-saving toxin removal modality for patients who have overdosed on traditionally non-dialyzable drugs

## Future Work

- Test multiple toxins in ECMO circuit with animal blood
- Explore a modular approach with different filters
- Patent technology and explore animal testing

We will explore testing with animal blood to further improve clinical relevance. We predict that this will reduce the error between the potential and target removal rates because the filter ultrafiltration coefficient (which was used to calculate target flow rates) was given for blood at 37 °C.

## References/Acknowledgments

1. Gurnam, D et al. (2017). Clinical Toxicology 56(10), 1072-1254.   
 2. Wang, G et al. (2015). Journal of Medical Toxicology, 7(1), 65-69.   
 3. REVACLEAR Dialyzers - Baxter Healthcare. Retrieved May 4, 2018.   
 4. Madan, C et al. (2013). Journal of Toxicology, 7(1), 105-116.   
 5. We would like to thank all of our mentors for their knowledge, assistance, and dedication to our success. Thanks to Dr. Zhongjun Wu for providing us with a lab space and materials for testing. We would also like to thank Carmen Carisano and Dr. Neil Blough of the UMD Chemistry Department for their assistance with UV-visible spectroscopy. Finally, thank you to the Fischell Department of Bioengineering for sponsoring this project.

## **High-Flux Hemofiltration System for Rapid Toxin Removal**

Morgan Hoffman, Daniel Hopkins, Morgan Janes, Milan Patel, and Manaahil Rao

Acute poisoning is a clinical problem that affects 2.16 million people each year. Hemofilters, which are designed to remove fluid from the blood during cardiac bypass, can also be used to filter toxins from the bloodstream in certain toxic ingestions. Unfortunately, current hemofilters lack the filtering capacity for many traditionally non-dialyzable toxins, resulting in limited clinical applicability for critical ingestion patients. Commercially available hemofilters lack adequate surface area and are unable to filter blood at high enough rates to remove toxins with a large volume of distribution or high protein binding fraction. Extracorporeal membrane oxygenation (ECMO) is an adjacent technology designed to treat heart and lung failure that circulates blood at high flow rates (4-5 L/min). While ECMO is unable to provide toxin removal, in recent years it has been increasingly used to offer hemodynamic support for critically ill patients suffering from toxic overdose. The goal of this project was to develop an ECMO-compatible hemofiltration system to facilitate rapid and efficient acute toxin removal at high flow rates. By increasing the overall surface area and incorporating the system directly into an ECMO circuit, we sought to overcome traditional challenges with hemofilters to enable rapid filtration of traditionally non-dialyzable toxins. Our team developed a prototype toxin filtration system by creating a parallel “circuit” of eight connected hemofilters. This system can support an input flow rate of 4 L/min, and it was able to remove the non-dialyzable toxin flecainide from saline at an improved and clinically relevant rate. Our final results show a 16-fold increase in the removal rate, with potential for a 21-fold increase, in comparison to traditional hemofiltration. The clinical contribution of this project is a robust, time-saving toxin removal modality for patients who have overdosed on traditionally non-dialyzable drugs.

# MR Surgery: Mixed reality prostate surgery from patient derived MRI scans

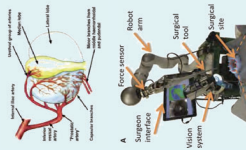
Christian Haryanto, Anjana Hevaganinge, Hannah Horng, Madeleine Noonan-Shueh

Advisors: Dr. Minhaj Siddiqui, University of Medicine, School of Medicine, Dr. Axel Krieger, Department of Mechanical Engineering, University of Maryland, Dr. Lan Ma, Department of Bioengineering, University of Maryland

## Background & Motivation

**PROBLEM:** Prostate cancer currently affects millions of Americans and often requires radical prostatectomy as treatment. Residents in urology as well as robots used in surgery require guidance in what tissue requires resection without harming surrounding organs.

**OUR SOLUTION:** Our aim is to develop a digital 3D model of prostate anatomy be used to generate a simulations in augmented reality (AR) and virtual reality (VR) that can train and guide both surgeons and the STAR robotic arm that is currently being developed to perform automated surgery.



## Objectives

1. Generate an augmented reality overlay for video feeds of prostate resection that allow user interaction with display of the prostate and surrounding anatomy
2. Generate a virtual reality simulation which can model the tissue deformation of the prostate and surrounding tissue for pre-surgical planning purposes.
3. Integrate the two simulations to provide training data and real-time surgical guidance for prostate resection.

## Approach

To implement our objectives in both augmented and virtual reality, we used **freely available software and toolkits:**

- **Unity:** A cross-platform engine originally developed for game development, but also now the main platform for mixed reality
- **C#:** The coding language for this software is C#, written in **Visual Studio**
- **Vuforia:** A software development toolkit used to easily implement augmented reality using automated detection of feature points
- **Blender:** An open-source 3D computer graphics software used to develop 3D textured models in games, animation, art, and more.

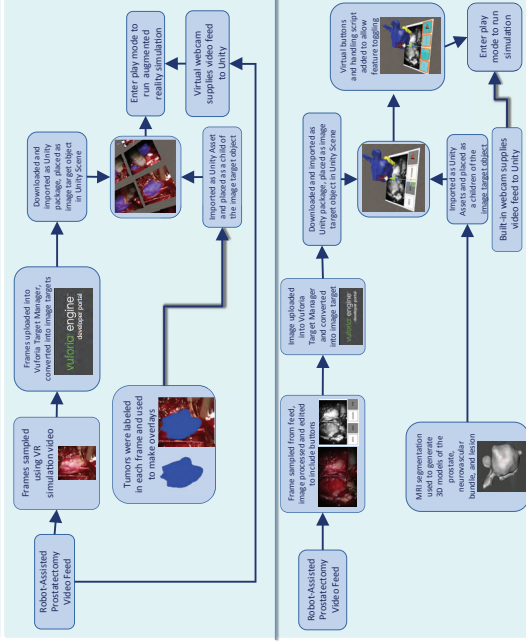


To complete simulations and verify our results, we used **licensed software**

- **MATLAB:** A numerical computing environment that allows for matrix manipulations and finite element analysis
- **Creo:** A computer aided design (CAD) software that allows the prediction of physical behavior using finite element analysis

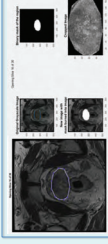


## Methodology: AR Simulation



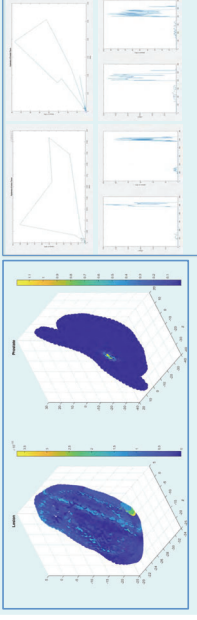
## Results

### AUGMENTED REALITY RESULTS



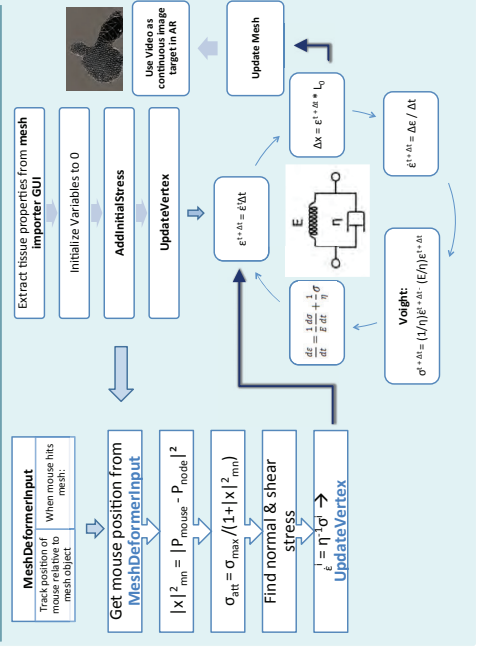
**Left:** 3D models of the prostate, neurovascular bundle, and lesion overlaid onto an image target with virtual buttons.  
**Middle:** Automated blue overlay over the prostate in a video feed of a robot-assisted prostatectomy  
**Right:** Automated red overlay of the VR prostate deformation

### VIRTUAL REALITY RESULTS



**Left:** Modulus displacement map plotted on the mesh of lesion (Top) and Prostate (Bottom)  
**Middle:** Stress (kPa) strain hysteresis loops obtained from simulation  
**Right:** Stress (kPa) and strain graphs over time for lesion and prostate

## Methodology: VR Simulation



## Future Directions

### NEXT STEPS

- Evaluate the practicality and usability with Likert survey
- Integrate the AR and VR simulations into a single platform
- Use patient specific video feed

### ETHICAL IMPLICATIONS

- Obtaining medical files for calibration must be done with the proper approval
- By improving the pre operative planning, the rate and cost associated with correctional procedures will decrease

### CONCLUSIONS

- Here we demonstrate a proof of concept for soft tissue modeling with native properties using Unity, a traditional game engine, for medical applications.

## References

1. Hoyt, Kenneth, et al. "Tissue elasticity properties as biomarkers for prostate cancer." Cancer Biomarkers 4:4-5 (2008): 213-225.
2. Koren. "Defkit Deformable Toolkit" Unity-Asset Store (2015).
3. Mohamed, Ashraf, Christos Davatzikos, and Russell Taylor. "A combined statistical and biomechanical model for estimation of intra-operative prostate deformation." International Conference on Biomedical Computing and Computer-Assisted Intervention. Springer, Berlin, Heidelberg, 2002.
4. Shadmehr, A., Decker, R. S., Opfermann, J. D., Leonard, S., Krieger, A., & Kim, P. C. (2016). Supervised autonomous robotic soft tissue surgery. Science translational medicine, 8(337), 337ra61-337ra64.

## **MR Surgery: Mixed reality prostate surgery from patient derived MRI scans**

Christian Haryanto, Anjana Hevaganinge, Hannah Horng, Madeleine Noonan-Shueh

Prostate cancer affects millions of Americans, and often requires a radical prostatectomy to remove both the prostate and the tumor to treat the cancer. Following the surgery, an anastomosis must be performed to replace the bladder and the urethra. Surgeons often have difficulty identifying where the prostate and surrounding anatomy are, and must take extreme caution not to damage other organs, including the neurovascular bundle. Our goal is to leverage recent developments in mixed reality to create surgical guidance and training data for surgeons to more effectively complete surgery. Our models use virtual reality to simulate the mechanical stresses that cause deformation of the prostate and other organs during surgery. This data can be used to generate data for augmented reality simulations that allow automated tracking and labeling of the prostate, as well as an interactive display of a patient-derived 3D model of the prostate. Our simulations can reduce the cost of this vital surgery and increase the quality of patient care by providing surgical guidance during prostatectomy.

# Portable Cardiac Stimulator For Electrophysiological Studies

Andrew Amick, Larry Feldman, Shireen Khayat, Paula Kleyman, Amanda Marques

Advisors: Rafael Jaimes PhD, Children's National Hospital and Professor Shawn He, PhD, Department of Bioengineering, University of Maryland

## Abstract

Electrophysiological Studies (EPS) are used to characterize the function of a heart. Currently, researchers use dated cardiac stimulators for EPS, that are inaccessible, bulky, and difficult to use. We aim to replicate and improve the functionality of the cardiac stimulator currently used at Children's National Hospital with a microcontroller as a more cost effective and intuitive alternative in order to replace the antiquated system.

## Background

- A variety of cardiac stimulators are used to conduct EPS.
- **Bloom DTU-215B** : Model currently used by Children's National (Fig. 1)
- **Micropace ORLab™**: Current State-of-the-Art (Fig. 2)



Figure 1: Bloom DTU-215B Model

Existing models are **expensive**, **large**, and **complicated**, so we aim to replace them utilizing accessible and ubiquitous materials



Figure 2: Micropace ORLab™

## Methods

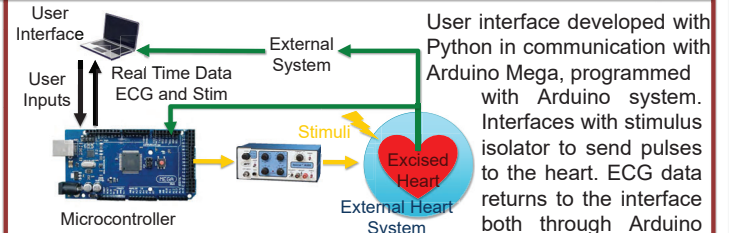


Figure 3: Schematic describing the system and flow of information, including as ECG and Stimulus data

User interface developed with Python in communication with Arduino Mega, programmed with Arduino system. Interfaces with stimulus isolator to send pulses to the heart. ECG data returns to the interface both through Arduino and from external system for verification

## Objectives

We aim to use a microcontroller to create a **inexpensive**, **portable**, and **intuitive** device that can be used to conduct electrophysiological studies. It must be compatible with software and hardware used at Children's National Hospital and perform all necessary functions to conduct animal studies more efficiently and accurately than the current Bloom Cardiac Stimulator.

## Results

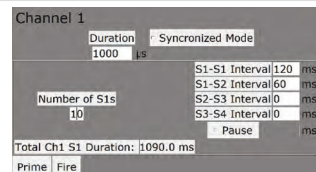


Figure 4a: GUI with example user defined settings entered.



Figure 4b: Expected corresponding stimuli

These images were obtained during an animal study conducted at Children's National Hospital. User defined parameters were set in the GUI to emit 1000μs long stimuli at an interval of 120ms, then an additional stimulus at 60ms as shown in Figure 4a. Based on the set parameters, it is expected that graphically the stimulus would look as depicted in Figure 4b. A screenshot of the live plot on the user interface, shown in Figure 5, was obtained and compared to the ECG results produced using the current IOX2 software from emka TECHNOLOGIES to assess accuracy, shown in Figure 6. Throughout experimentation it was found that our device had a minimum interval of capture at 30ms.

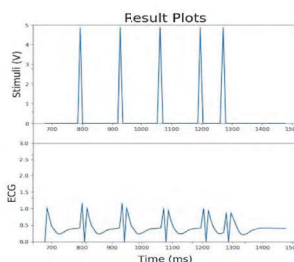


Figure 5: Screenshot of live plotting of stimuli and ECG on user interface.

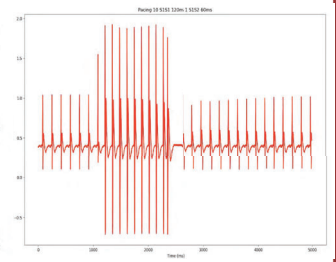


Figure 6: Based on the ECG results, we can verify that the stimuli was successful in pacing the heart.

## Conclusions

- Through an analysis chart (Tab. 1), it was determined that our device was successful in improving upon existing technology in the three critical fields addressed.
- Additionally, our cardiac stimulator experimentally showed a

Model	Cost	Size	Usability
Bloom	\$1000+*	~11 kg	Difficult
ORLab	\$45000+	5.3 kg	Difficult
Ours	<\$50	0.037 kg	Easy

Table 1: Comparison between devices in three fields

minimum interval of capture at 30 ms, an improvement upon the Bloom's 50 ms.\*\*  
- Device is not only comparable to the Bloom, but in some ways it is an improvement

\*used, \*\*limited experimental testing

## Ethical Implications

### Intellectual Property

- Open-source and Accessible Materials
- Guide to developing this device will be made publicly available
- Promotes collaborative research in the field, leading to the development of new technologies

### Ethical Implications

- Device is not inherently dangerous, but is a prototype and not approved for clinical uses
- Thorough disclaimers are needed to prevent misuse



## Future Work

Improvements upon the developed cardiac stimulator include increasing the display rate of the live plot, including multiple channels, and developing wireless Bluetooth capabilities. The ultimate goal for this device is use in clinical settings, and the research described above has paved the way for such a device to exist.

Special Thanks to Dr. Lan Ma, Dr. Yang Tao, and Damon McCollough

## **Portable Cardiac Stimulator for Electrophysiological Studies**

Andrew Amick, Larry Feldman, Paula Kleyman, Amanda Marques, and Shireen Khayat

Heart function can be characterized and analyzed using electrophysiology (EP), a branch of biology that pertains to the propagation of ion current in the heart. EP studies utilize cardiac stimulators, a device that outputs programmed electrical pulses, to initialize and study impulse propagation through different areas of the heart by inducing arrhythmias. When combined with quantification or visualization of the changing electric potential in the heart, EP studies provide insight on disease pathologies. EP studies can also be used to assess the effects of different substances on heart function, including environmental toxins and newly developed pharmaceuticals. Current cardiac stimulators are very large, bulky devices that are difficult to move between rooms and high cost, making it undesirable, but necessary to have to purchase a separate device for each room. Due to the significant impact these studies have, there is a need to increase the usability and portability of the cardiac stimulator while making them affordable and efficient. To do so, we have created a prototype of a portable external cardiac stimulator that mirrors and improves the functionality of the cardiac stimulator currently used at Children's National Hospital by utilizing a microcontroller as a more cost effective and intuitive alternative. Our device is compacted to allow for quick transport, thereby eliminating the need and costs associated with having multiple devices. It maintains the basic, most used functions of current cardiac stimulators, allowing user regulation of different pulse parameters and offering an option for synchronized pulsing that utilizes real-time ECG data to determine ideal pulse intervals. The device includes user interface software usable on any personal computer that regulates a microprocessor controlled electrical output. The output is designed to interface with a stimulus isolator that isolates, modifies, and delivers the precise signal through leads that attach to the heart. The microprocessor is also able to read in the pulses it outputs, as well as the surface electrocardiogram signals provided by an amplifier. It then can send the values to the interface for real-time plotting. Our portable cardiac stimulator will make EP studies more accessible and less laborious for researchers and clinicians.

# Noise-Reducing Electromagnetic Latch System for NICU Isolettes

Jillian Carter, Austin Goncz, Sara Merlock, Samuel Mircoff, Blair Smith  
 Advisors: Dr. Yu Chen, Fischell Department of Bioengineering, UMD and Dr. Rose Viscardi, UMCC  
 Special Thanks to: Allen (Yalun) Wu, Michael Restaino, Gary Seibel, Dr. Yang Tau

## Motivation

**Background:** The Neonatal Intensive Care Unit (NICU) is a section of the hospital where high-risk infants are sent to be continuously monitored. Many of these high-risk infants are born prematurely, or before 37 weeks<sup>1</sup>. Premature infants are more vulnerable to hearing loss due to underdevelopment. Current noise reduction solutions focus on total sound and not solely sound from the doors.

**Problem Statement:** The current opening and closing mechanism on isolette doors reaches noise levels of up to 90 dB, while the recommended level for the NICU is 45 dB<sup>2</sup>.



Figure 1. Original latch mechanism

### Objectives

1. Redesign the port-latch mechanism of the isolette such that noise output upon opening or closing is 45 dB maximum
2. Keep the opening of the doors as hands free and quick
3. Design the new mechanism such that it can be easily integrated to current models and is low cost

## Methods



**The Problem:** The current plastic latch mechanism emitted a loud clicking noise.  
**Design Concept:** Remove the latch and add an electromagnet and sensor.

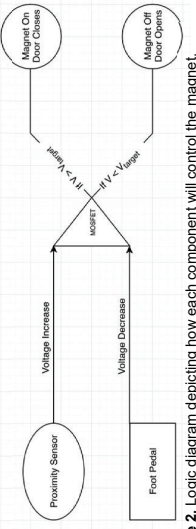


Figure 2. Logic diagram depicting how each component will control the magnet.

**Circuit Design & Code:** Figure 2 was adapted into a circuit and used to develop the Arduino code (See Fig. 4). Specifications for the circuit components:  
 • Electromagnet: At least 5 kg holding force to hold ~1 kg door

• Proximity sensor: Sense at least 20 cm  
**Design Housing Unit:** Housing unit for the magnet and sensor was designed to be easily integrated onto the current isolette. Polycarbonate was used to house a piece of metal to the porthole door.



Figure 3. CAD design of the housing unit

**Material Selection:** (1) The material around the porthole needed to be cheap, noise resistant, and compatible with sanitation methods. (2) To ensure that the electromagnet did not heat up, a material was needed with low specific heat that was also safe. Cork was chosen due to its specific heat of 1.9 kJ/(kg-K).

**Testing:** The noise output levels of the opening and closing of the door were measured using the app DecibelX in a room with noise level similar to the NICU.

## Final Design

Primary Materials		Final Prototype	
Arduino Uno	Adrafruit 5V Proximity Sensor	EPDM Rubber Foam Lining	3D Printed Housing Unit

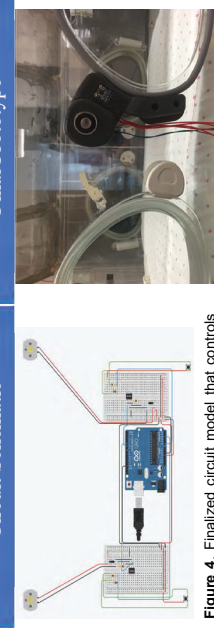


Figure 4. Finalized circuit model that controls the electromagnet that will hold the porthole closed. Sensor not included, no representative model available in the software used.

## Results

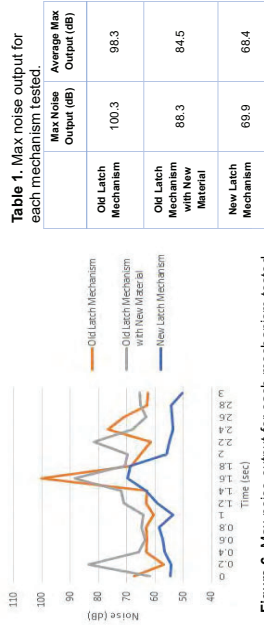


Figure 5. Prototype design mounted on isolette next to original latch.  
 Figure 6. Max noise output for each mechanism tested. The results show that the noise is reduced by replacing the latch mechanism. They also show that the new material reduces the noise output.

Once the code was finalized the electromagnetic field of the magnet was modeled using MATLAB.

The flux density, which is proportional to the force generated by the field, is greatest within a few millimeters of the face of the magnet and decreases rapidly.

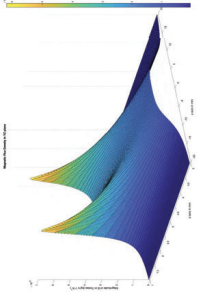


Figure 7. Adapted from a third party MATLAB function, the figure above represents the magnetic flux density in Tesla, where the face of the magnet sits in the XY plane, and the field is therefore in the Z plane.

## Ethical Implication

- ~12% of babies are born premature<sup>1</sup>
- ~4 million births a year means ~480K premature
- 10-15% babies go to the NICU<sup>3</sup>
- ~10-15% of babies go to the NICU<sup>3</sup>
- ~400K-600K babies go to the NICU a year

## Conclusions

- The new latch design did reduce the maximum noise output compared to the current latch mechanism and had a hands free and quick open. The device was easily integrated, but was not as low cost as intended.
- Many other factors contribute to the ambient decibel range in the NICU. This latch system eliminates any major rise from the baseline, but ambient noise remains around 50-60dB. Thus reducing this to under 50 dB likely requires redesign of the environment itself.
- The team learned that working with devices for infants allows a lot of room for creativity, but it also lends many limitations to design possibilities due to the fragility of these patients.

## Future Work

- Enhance mechanism for two door operation
- Updated build with more robust parts and finish to allow for autoclaving
  - IP69K rated parts and housing material
  - Encase sensitive components in potting compounds
- Six Sigma Analysis
- Implement fail safe/fail secure circuitry
  - In the event of power loss, magnet should remain on but be operable with a tight pull so doors are not hanging open
- Revisit circuit design with smaller or more efficient hardware to reduce potential heat damage and provide maximum visibility into the isolette

## Significant References

1. Lucile Packard Children's Hospital. (n.d.). Prematurity. Stanford Children's Health. Retrieved from <https://www.stanfordchildrens.org/en/topic/default?id=prematurity-126-102401>. S. L. (2018). Noise level in neonatal incubators: A comparative study of three models. *International Journal of Pediatric Otorhinolaryngology*, 107, 150-153.
2. Knispel, S. (n.d.) What Parents Should Know About NICU Care. Meredeth Corporation. Retrieved from <https://www.parenting.com/articles/nicu-care>.

## **Noise-Reducing Electromagnetic Latch System for NICU Isolettes**

Jillian Carter, Austin Goncz, Sara Merlock, Samuel Mircoff, Blair Smith

Recent research has indicated that decibel levels above 45 dB can impact normal neurological development in premature neonates. It was discovered that this level of noise, and more, is created in the Neonatal Intensive Care Unit (NICU) by the monitoring instrumentation, human activity, and the opening and closing of portholes on isolettes. To mitigate the potential effects of ambient noise, NICU staff now separate infants into individual, quieter rooms. However, the excessive level of noise created by the opening and closing of the current porthole latch mechanism still remains a problem. Our group has designed a new electromagnetic latch system that will allow the NICU staff to gain immediate access to the child in case of an emergency, while generating less noise than current latch mechanisms. The new mechanism is controlled via a foot pedal, proximity sensor, and Arduino Uno microcontroller. The proximity sensor detects when the porthole door is nearly closed and activates the electromagnet, locking the door shut while still allowing manual access in case of emergency. The foot pedal then provides a direct, hands-free mechanism to turn off the electromagnetic, and open the isolette door quickly. The electromagnet and proximity sensor are retrofitted onto the current isolette design via a custom 3D printed housing unit that attaches in place of the original latch. This new mechanism decreased max noise output while opening and closing the doors by over 20 dB, but did not lower it to the goal of below 45 dB. This could be due to ambient noise in the NICU, which ranges from 50-55 dB at baseline. Further work for this design includes making the circuit more robust and providing a finish that would be more suitable for sterilization



# Erythrocyte Mediated Angiography Verification with Phantom Eye

Danielle Firer, Matthew Kim, Rachel Luthcke, Richard Silcott, Drew Vogel

Clinical Mentor: Dr. Osamah Saeedi, University of Maryland Medical Center

Faculty Advisor: Dr. Giuliano Scarcelli, Robert E. Fischell Department of Bioengineering, University of Maryland

## Clinical Need

### Motivation:

Glaucoma, Diabetic Retinopathy, and Age-Related Macular Degeneration are three leading causes of blindness linked to impaired ocular blood flow [1] [2] (Fig. 1)

### Problem:

- Ocular blood flow is a potentially important biomarker for early onset ocular pathologies.
- Current measurement techniques depend on erythrocyte mediated angiography (EMA) using a Heidelberg Retinal Tomograph (HRT) (Fig. 2)
- HRT uses a patient's native cornea for magnification, but the assumption that its dimensions does not affect angiography measurements is not well characterized.



Figure 1. Prevalence of ocular pathology.

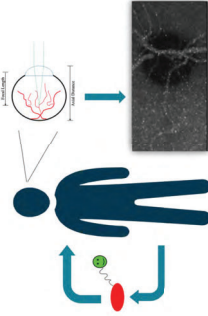


Figure 2. EMA imaging chain.

### Objective:

This project aims to create a device to investigate HRT measurements for multiple lens strengths and axial distances by comparing incident red blood cell speed.

## Phantom Eye Concept

### Our Approach:

Our phantom eye is a testing platform to assess the HRT's ability to measure ocular blood cell speed for different lens powers and axial distances. Two main components on our 3D printed phantom provide precise control of these parameters:

- Lens position** - Triangular lens holder slides into a slot that centers the lens at a fixed x, y, and z position.
- Axial distance** - 3D printed capillary holder slides into a rack with sawtooth indents from 18mm to 32mm at 2mm increments.

Silicon tubing with inner diameter of 100µm was used to model an ocular blood vessel.

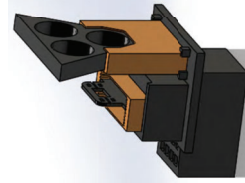


Figure 3. Phantom diometric view. Capillary holder at 22mm.

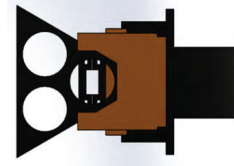


Figure 4. Bottom lens centered and aligned with viewing window. (Lenses omitted)

## Data Collection

### Lens Alignment (Fig. 5):

- Lens holder clamped into a calibrated laser breadboard
- USAF chart group 6 centered in field of view
- Capture image before and after resetting the triangular lens holder
- Measure change in smallest resolvable element and x-y shift (Fig. 7-8)



Figure 5. Lens alignment characterization setup, provided by Dr. Giuliano Scarcelli

### Angiogram Collection (Fig. 6):

- Phantom eye clamped onto HRT chinrest
- Syringe loaded with fluorescent labeled blood cells
- Tubing fixed onto capillary holder and placed into rack
- Syringe pump turned on and set to 0.005 mL/min flow rate
- Align HRT camera and collect 10 sec angiogram
- Repeat for next rack position and each lens
- Manually track blood cells in ImageJ to estimate speed (Fig. 9-10)



Figure 6. Angiogram collection set up on HRT

## Results

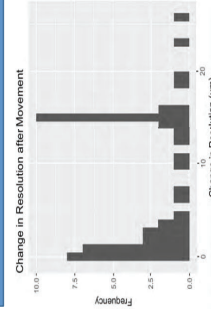


Figure 7. Histogram of change in size of smallest resolvable element after resetting lens holder.

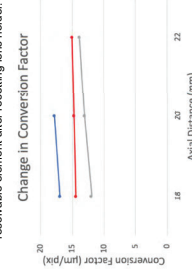


Figure 9. Measured conversion factor at each axial distance and lens power.

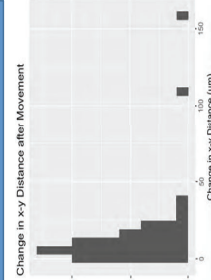


Figure 8. Histogram of change in x-y position after resetting lens holder.

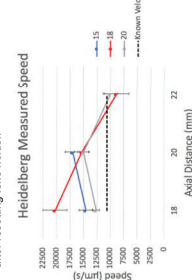


Figure 10. Measured blood cell speed at each axial distance and lens power.

## Discussion

### Conclusions:

- Resolution changes from resetting the lens could be eliminated by adjusting the HRT camera and x-y shifts were minimal.
- The increase in conversion factor as axial distance increased and focal length decreased was expected
- Surprisingly, the measured velocity was within one standard deviation of the expected speed (10610.33µm/s), only at an axial distance of 22mm.
- Further testing is needed to comprehensively characterize the effect of axial distance and lens power on HRT image quality.

### Ethical Implications:

- Pave the way for more quantitative and personalized diagnosis of ocular pathologies through impaired blood flow.
- Positively impact the accuracy of diagnosing major causes of blindness worldwide.
- Specifically making a positive impact on the early diagnosis and monitoring of patients who have Glaucoma, Diabetic Retinopathy, or Age-Related Macular Degeneration.
- Not a risk to patients as our device will not be in contact with human subjects.

### Future Work:

- Develop more physiologically accurate capillary tube (inner diameter, convolution, and material)
- Add lower powered lenses
- Apply of pulsatile flow through the capillary tube
- Refine procedure to diagnose ocular pathology based on impaired blood flow

### Special Thanks To:

Dr. Giuliano Scarcelli, Dr. Osamah Saeedi, Lakyn Mayo, Dr. Anant Agrawal

### References:

- Common Eye Disorders. (2015, September 29). Retrieved from Centers for Disease Control and Prevention website.
- Dunaief, J. (2018, October 24). Eye Diseases that Can Cause Legal Blindness. Retrieved from BrightFocus Foundation website.
- Cioji, I., Gruppeta, S., & Hunjens, B. (2015). The effects of ocular magnification on Spectralis spectral domain optical coherence tomography scan length. Graefes Archive for Clinical and Experimental Ophthalmology, 253(5), pp. 733-738. doi: 10.1007/s00417-014-2915-9

## **Erythrocyte Mediated Angiography Verification with Phantom Eye**

Danielle Firer, Matthew Kim, Rachel Luthcke, Richard Silcott, and Drew Vogel

Recent studies have shown that impaired ocular blood flow is implicated in the progression of Glaucoma, Diabetic Retinopathy, and Age-Related Macular Degeneration, three of the leading causes of blindness worldwide. To facilitate early detection of these pathologies, researchers have developed techniques for measuring ocular blood flow. One of the primary methods is erythrocyte mediated angiography (EMA). When performing EMA, blood is extracted from the patient and mixed with Indocyanine Green (ICG) to label the red blood cells by fluorescence. The ICG-labeled blood sample is reintroduced into the patient's body and a Heidelberg Retinal Tomograph (HRT) is used to capture an angiogram, where the ICG-labeled blood cells appear as brighter pixels. These cells are used to measure blood cell speed and track ocular blood flow in all patients. When imaging with HRT, the patient's native cornea is used for additional magnification; however, corneal dimensions and vessel position in the eye vary across all people. This study investigated the assumption that axial distance (AD) of the blood vessel and/or the focal length (FL) of the lens does not affect HRT images. Three FL (15mm, 18mm, 20mm) and three AD (18mm, 20mm, 22mm) were tested. For all trials, blood flow was fixed at a rate of 0.005mL/min and cell speed of 10610.33 $\mu$ m/s. Only trials collected at an AD of 22mm were within one standard deviation of the expected speed; however, the 15mm lens could not focus on the vessel at 22mm. Image resolution increased as AD increased, but decreased as lens FL increased. Our device was able to successfully investigate the impact of lens strength and axial distance on HRT measurements by comparing incident red blood cell speed. The application of this system has the potential to accelerate research related to the development of more accurate diagnosis and monitoring of major causes of blindness worldwide.

# SpiCast - Safe Transportation for Pediatric Patients with Femur Fractures

Deven Appel, Danya Chowdhury, Shweta Roy, Richard Sellars

Advisor(s): Dr. Lester Schultheis, Fischell Department of Bioengineering, University of Maryland / Dr. Matthew Oetgen, Children's National

## Introduction

### Problem

Pediatric femur fractures are the second most common long bone fractures in kids. Nineteen out of every hundred-thousand children in the United States experience femur fractures every year.<sup>1</sup> Within the past year, an estimated 14,800 children between the ages of 0 to 11 had a femur fracture.<sup>2</sup> The most common form of treatment for children under the age of five is immediate spica casting.

Spica casts immobilize the child at the hips as its bound to maintain a sixty degree hip abduction, thirty degree hip flexion, and forty-five degree bend at the knees. Due to these set angles, patients' legs are positioned in such a way that the knees are pointed to each side of the body. This positioning causes the legs to be farther apart than in the normal seated position. Everyday car seats do not provide the space, comfort or ease for spica cast patients. This project focuses on finding a solution to facilitate transportation for spica cast patients.

### Existing Intervention

The Hippo car seat is the only car seat that complies with Federal Motor Vehicle Safety Standards and is also approved for patients with spica casts. As of 2015, the Hippo car seat is no longer being manufactured.<sup>4,5</sup> Furthermore, older models that were produced range in price from \$500-\$900. The Hippo car seat is bulkier than a normal car seat and it is harder to install. Since recovery time for a pediatric patient with femur fractures is no longer than 12 weeks, buying an entirely new car seat is not practical.

### Proposed Intervention

Our solution for this problem is to create an attachment that can be inserted into the regular car seat of the patient. This attachment, the SpiCast, will be inexpensive, feasible to reproduce, and comfortable for the patient.

## Specifications

<ul style="list-style-type: none"> <li>Child</li> <li>Age: 1-3 year old</li> <li>Weight: 11-25 kg</li> <li>Waist Circumference: 21"</li> <li>Waist to Knee Length: 11"</li> </ul>	<ul style="list-style-type: none"> <li>Spica Cast</li> <li>60° hip abduction</li> <li>30° hip flex</li> <li>45° bend at the knees</li> <li>Made with fiberglass</li> </ul>
<ul style="list-style-type: none"> <li>Car seat</li> <li>Top is 1" above child's head</li> <li>Hip room: 14" interior</li> <li>Seat pan: 12.5" deep</li> <li>5 Point Strap System</li> <li>Placement</li> </ul>	<ul style="list-style-type: none"> <li>Forces</li> <li>Force in car accident - 668 N with stopping distance of 2 meters</li> <li>Force sitting in cast - 120 N</li> <li>G forces: 20-30 G's</li> </ul>

## Methods

<ol style="list-style-type: none"> <li>Place 15 lbs of lentils into a vacuum sealable bag.</li> </ol>	<ol style="list-style-type: none"> <li>Fit patient within bag and vacuum air out.</li> </ol>	<ol style="list-style-type: none"> <li>Lay overlapped fiberglass on mold. Set for 20 minutes.</li> </ol>
<ol style="list-style-type: none"> <li>Spray expandable foam within parchment-lined 1' by 1' box, with smooth 2" layer.</li> </ol>	<ol style="list-style-type: none"> <li>Set fiberglass mold and wait 8 hours for curing.</li> </ol>	<ol style="list-style-type: none"> <li>Size foam insert to patient car seat and install.</li> </ol>

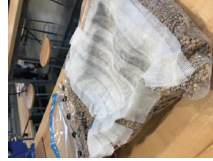


Figure 1. Fiberglass laid out on lentil mold.



Figure 2. Expandable foam with fiberglass.

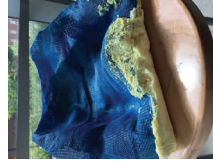
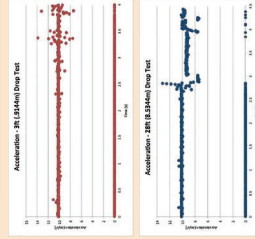


Figure 3. Finished expandable foam mold.

## Results



Figures 4 and 5. Acceleration data was plotted in Excel. Data was taken at 3ft and 28ft drop. Minimum values are 7.37 and 7.34 m/s<sup>2</sup> for 3ft and 28ft respectively.



Figure 6. (top-left, clockwise) Parametric scan of car seat with model insert; electronics circuit with Arduino ADXL345; OpenSource Wireless Shields; Arduino physical setup; sensor on car seat with model baby.

## Conclusions

In the process of making the SpiCast, we have developed a prototype that will allow patients in spica casts to use regular car seats. This prototype is both tailored to the individual patient and their car seat, it is 1/27<sup>th</sup> the cost of the Hippo car seat, and is easier to install. While creating this product, the team was able to identify a clinical problem, brainstorm different approaches, and work towards a single solution after several rounds of prototyping. During this process, we learned the significance of trial and error, and realized how crucial it is to obtain the actual measurements of the patient and car seat in order to finetune our design. We see promise in the vacuum bag mold design for a final model. After the design was finalized, a drop test was performed to evaluate the impact forces on the child. The results showed that the acceleration on the baby was reduced by 2 m/s<sup>2</sup> with the car seat, whereas the acceleration drop on the baby is consistent between a 3 ft and 28 ft drop with our setup. Further tests from this pilot can verify efficacy and lead to eventual approval with Federal Motor Vehicle Safety Standards. Utilizing the SpiCast shows promise as a safer alternative to currently used methods.

## Ethical Implications

- Reduces parental strain
- Reduces financial burden - \$500/900 → \$33.23
- Improves safety and allows for proper healing
- Easier installation and provides comfort for injured children
- Tailored attachment fit to needs of each patient
- Reduces waste

## Future Work

- Material Exploration for vacuum-sealed bag, lentils, and expandable foam
- 3D printed mold for car seat insert made from polypropylene
- Further acceleration testing with developed electronics setup
- Crash Testing with SpiCast to conform to Federal Motor Vehicle Safety Standards
- IRB Testing with SpiCast inserts

## References and Acknowledgement

- Special thanks to our faculty advisor, Dr. Lester Schultheis, our clinical advisor, Dr. Matthew Oetgen, and our professors, Dr. Ying Tao and Dr. Lan Ma, for their guidance throughout the project.
- Hilton, R. Y., Lincoln, A., Crockett, M. M., Spenseller, P., & Smith, G. (1989, April). Fractures of the femoral shaft in children: incidence, mechanisms, and sociodemographic risk factors. Retrieved from <https://www.ncbi.nlm.nih.gov/pmc/articles/PMC1326000/>
  - Child State. (n.d.). Retrieved from <https://www.childstate.gov/americanchildren/tabletop1.asp>
  - Rewers, A. (2005, 05). Childhood Femur Fractures. Associated Injuries, and Sociodemographic Risk Factors. Retrieved from <https://www.ncbi.nlm.nih.gov/pmc/articles/PMC1326000/>
  - 49 CFR 271.213 - Standard No. 213: Child restraint systems. (n.d.). Retrieved from <https://www.ecfr.gov/current/title-49/chapter-I/subchapter-B/part-271/subpart-213/section-271.213>
  - RETIRED PRODUCT. (n.d.). Retrieved from <https://us.bibox.com/retired/mammoth/>

## **SpiCast - Safe Transportation for Pediatric Patients with Femur Fractures**

Deven Appel, Danya Chowdhury, Shweta Roy, Richard Sellars

Pediatric femur fractures are the second most common long bone fracture in kids. Nineteen out of every hundred-thousand children in the United States experience femur fractures every year. Within the past year, an estimated 14,600 children between the ages of 0 to 11 had a femur fracture. These fractures can be as a result of birth, hip dysplasia, or due to unintentional falls and accidental injuries. Treatment varies and depends heavily on the child's age. However, the common form of treatment for children under the age of 5 is immediate spica casting, which is an orthopedic cast that immobilizes the hip or thigh.

Everyday car seats do not provide the space, comfort or ease for spica cast patients. Although spica casts are the best method of treating children with femur fractures, they are extremely inconvenient, especially when it comes to transporting these children from place to place. Our team, ARCS Capstone, has created an attachment that can be inserted into the regular car seat of the patient, to be inexpensive, feasible, and comfortable. The prototype was created using an assortment of materials, including a vacuum-sealable bag, expandable foam, and fiberglass. The final product consists of a foam attachment that is tailored to the child and their respective car seat. After finalizing the design, a drop test was performed with the insert attached to a car seat to evaluate the impact of a fall on the child and car seat. From these results, we found that the acceleration on the baby was reduced by  $2 \text{ m/s}^2$  with the carseat, however, the acceleration drop remained consistent between a 3 ft and 28 ft drop with our setup. Overall, the proposed prototype offers several societal benefits such as reduced parental strain, reduced financial burden, and improved safety and comfort for injured children. Future work can be conducted that includes material exploration, consumer testing, and NHTSA confirmation.



# GaitMate: A Gait Monitoring Solution for Pediatric Cerebral Palsy

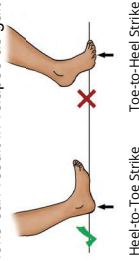
Tolulope Awosika, Nicole Duster, Jenny Katsnelson, Stacey Manuel, David Tucker

Advisors: Dr. Li-Qun Zhang<sup>1</sup>, Dr. Lan Ma<sup>1</sup>, Dr. Yang Tao<sup>1</sup>, Dr. Paola Pergami<sup>2</sup>, and Dr. Kevin Cleary<sup>2</sup>

1. Department of Bioengineering, University of Maryland 2. Children's National Hospital

## Background & Objective

- Cerebral palsy is neurological disorder of movement and posture that results from brain damage near time of birth that affects 1 in 323 children.<sup>1</sup>
- 1 in 323 children are diagnosed with cerebral palsy.<sup>1</sup>
- Out of all patients, 1 in 3 walk with the majority of their weight on the balls of their feet, as opposed to even weight distribution, eventually causing stiffness of leg muscles.<sup>2</sup>
- Current treatment for spastic cerebral palsy is through physical therapy and gait monitoring using external sensors and cameras.<sup>3</sup>
- Time between sessions can result in relapse as gait is not monitored constantly.

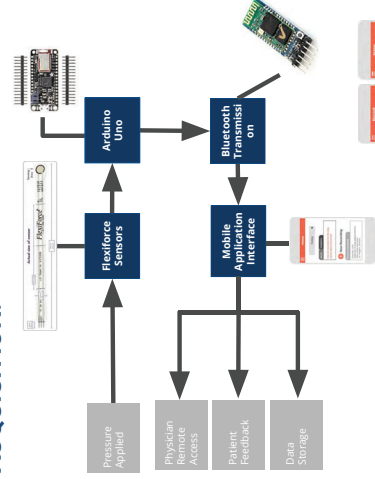


## GOAL:

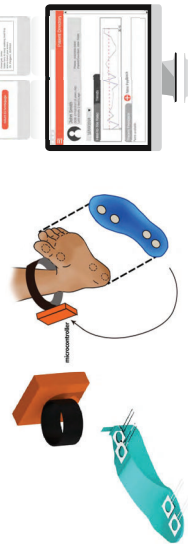
Improve patient physical therapy with increased data collection through a portable and wearable gait monitoring system.

## Methods

### DATA ACQUISITION:



### DESIGN CONCEPT:



## Results

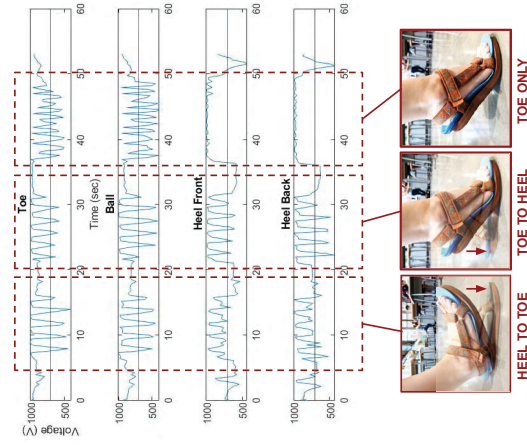


Figure 2. Sensor performance under known weights (5, 10, 15, 20, 25, 30 lbs represented in voltage vs time in second. Results suggest that sensors respond similarly to different weight ranges, suggesting they can easily be adapted towards different aged children.

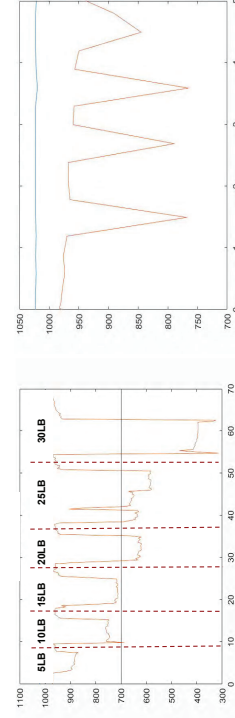


Figure 3. Sensor performance for short period of 5 seconds and small weight of 10 pounds shows relative speed in response time. Results suggest that the data acquisition system is fast enough to respond to a child walking in real time.



Figure 4. Screenshots of prototype mobile application featuring the main components of the patient interface. From left to right: navigation homepage, patient history, and sample recording screen.

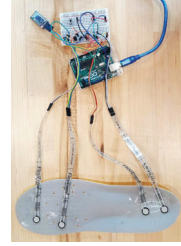


Figure 5. Picture of the pressure sole device prototype, connected to Matlab via Arduino for data collection and graphing.

## Discussion and Conclusion



- Lightweight ◊ High Pressure Range ◊ Bluetooth Compatible
- Portable ◊ Rechargeable ◊ Comfortable ◊ Biocompatible

## DISCUSSION:

In addition to our main goal, we were able to successfully meet all our initial design specifications:

- Lightweight:** Prototype weights only 7.58 oz, making it light enough for children to wear.
- Portable and Rechargeable:** Inclusion of a 9V battery and bluetooth module makes the device portable and allows it to be used for hours at a time before replacing the battery
- Biocompatible & Comfortable:** Using biocompatible materials for the soles makes the device safe, comfortable and easier to be approved by the FDA
- High Pressure Range:** As seen in Figure 2, the device is able to detect a wide range of pressures, allowing it to be easily adapted for children of all ages
- Cost effective:** The device only costs around 180 dollars. Given the device's ease of adaptability to different shoe sizes and weights, it can easily last throughout a child's progression through therapy. This makes it a cost effective alternative to the multiple trips to the physical therapy office which would otherwise be otherwise needed.
- Fast response time:** As seen in Figure 1, device can quickly adapt to different changes in gait.

## CONCLUSION AND IMPACT:

Overall, we have developed a successful prototype of the pressure sole gait monitoring system that will:

- Increase data collection and monitoring for accurate gait analysis and monitoring
- Reduce patient relapse between therapy sessions
- Improve accessibility due to low cost and simple user interface
- Children of all ages will be positively affected, benefiting from more accessible physical therapy. Physicians will also benefit from wireless data acquisition.

## Future Work

While we have demonstrated that our prototype can accurately measure and present results for an adult walking, there are a few areas we would like to further develop for the finalization of our product.

- Characterize and personalize device with children at varying stages of adolescence to validate product adaptability and ensure personalized care.
- Test device with both children who wear leg braces and those with regular shoes to optimize design for maximum comfort and decrease overall product size.
- Adapt sensors so they are more sensitive to faster motion such as running or fast walking.
- Further develop mobile app to be more kid friendly, interactive with live feedback, and with a secure data storage system for patient privacy.

## References

- Data and Statistics for Cerebral Palsy | CDC - Centers for Disease Control and Prevention, Centers for Disease Control and Prevention, 2018. <https://www.cdc.gov/ncbddd/cp/facts.html>.
- "Cerebral Palsy (CP)", Centers for Disease Control and Prevention, April 18, 2016. Accessed September 26, 2018. <https://www.cdc.gov/ncbddd/cp/facts.html>.
- Armand, Stephanie, Gerardo Decouzon, and Alice Bonnelly-Mazure. Current Neurology and Neuroscience 2018. <https://www.ncbi.nlm.nih.gov/pmc/articles/PMC5485760/>.

## **GaitMate: A Gait Monitoring Solution for Pediatric Cerebral Palsy**

Tolulope Awosika, Nicole Duster, Jenny Katsnelson, Stacey Mannuel, David Tucker

Cerebral palsy affects 3 out of every 1000 children in the United States. With spastic cerebral palsy comprising the majority of cases, many of these children suffer from abnormal gait patterns such as toe-walking which lead to future health issues such as stiffened leg muscles. While the current standard of care involves patients attending monthly physical therapy sessions, the relative infrequency of these visits often leads to relapses and therefore minimal progress. To facilitate for more frequent physical therapy for substantial gait improvement, a pressure-monitoring shoe sole has been developed. Four piezoelectric pressure sensors are attached to the top of a sole at strategic points which allow for one to distinguish between gait patterns. The sensors are then hooked up to an Arduino and Bluetooth to transmit data wirelessly to either a laptop or mobile application. After fabricating and testing the prototype, it has been concluded that the device is capable of tracking and recording an individual's gait in real time. It can detect both heel-toe and toe-heel walking and display distinct patterns. The response time of the device is rapid enough to accommodate a normal walking pace and is responsive to a wide range of applied weights. Further testing with a range of pediatric patients will be the next step in finalizing this product to provide the most accurate and comfortable product. Once on the market, the affordability and ease of use of this product will allow for patients to easily conduct physical therapy on a daily basis, increasing the likeliness of improved gait performance.

# Photodynamic Therapy as an Alternative to Tonsillectomy Procedures

**Justin Sylvers, Arley Wolfand, N. Zachary Rausch, Natalia Ochman, and Jason Chiang**  
 Faculty Advisor: **Dr. Huang Chiao Huang, Fischell Department of Bioengineering, University of Maryland**  
 Clinical Mentors: **Dr. Kevin Cleary, Dr. Avinash Eranki, and Dr. Rahul Shah, Children's National Medical Center**

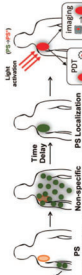
## Motivation

Tonsillectomies, a procedure performed to remove tonsils due to infection and sleep obstruction, are one of the United States' leading procedures in children. As of 2011 there were **530,000 performed each year**. Current tonsillectomy procedures, like cold-knife, electrocautery, and microdebrider techniques, have **high pain, risk of hemorrhage, and infection** associated with them.

## Background

Steps of photodynamic therapy (PDT):

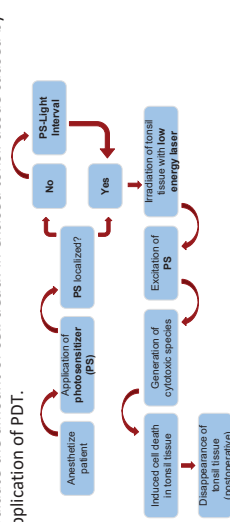
1. Inject/apply a **photosensitizing agent (PS)**
2. Allow for distribution to the target tissue
3. Use a **low-powered laser** to activate the drug
4. Generate cytotoxic species and **induce cell death** through mechanisms that vary with PS



## Objectives

**Experimentally validate** the use of photodynamic therapy (PDT) as an alternative approach to tonsillectomy procedures:

1. Evaluate the ability of the photosensitizer to **penetrate** excised tonsil tissue with varying concentrations and time considerations.
2. Evaluate the amount of **cell death** in excised tonsil tissue caused by application of PDT.



## Materials

- Excised tonsil tissue acquired from Children's National Medical Center with IRB approval.
- Liposomal Benzoporphyrin Derivative (L-BPD) in phosphate-buffered saline (PBS) ranging in concentration from 0.5 - 70  $\mu\text{M}$ .
- Precision LED Spotlight - Standard Range, 680 nm (Mightex).

## Drug Penetration Studies

- Cut excised tonsil tissue into equal cylindrical portions using a biopsy punch.
- Applied L-BPD solution and incubated.
- Cryosectioned samples and imaged with fluorescence microscopy (Ex/Em: 435/690 nm).



## Methods

### Cell Death Studies

- Four groups:
- (-)**BPD** (-)**Laser**, (+)**BPD** (-)**Laser**, (-)**BPD** (+)**Laser**, (+)**BPD** (+)**Laser**
  - Prepared cylindrical tonsil portions and applied drug as above using metrics with best penetration
  - (70  $\mu\text{M}$  BPD solution, 30 min. incubation)
  - Irradiated with 690 nm laser for 15 minutes at a height of 10cm to a fluence of  $\sim 75 \text{ J/cm}^2$
  - Cryosectioned samples, applied H&E stain, and imaged with BF microscopy.

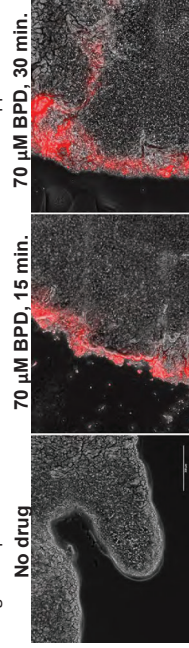


## Results

### Drug Penetration Results

Merged phase contrast and fluorescence images of sectioned tonsil tissue are shown below.

- 30 minute incubation resulted in greater penetration (distance from edge) than 15 minute incubation on average (155  $\pm$  112  $\mu\text{m}$  and 292  $\pm$  223  $\mu\text{m}$ ). Both were well below the target depth of germinal centers, 1-2 mm.
- As indicated by large standard deviations, the depth of penetration fluctuated significantly. This is attributed to uneven application of BPD solution, with greater penetration observed in areas closer to the location of application.



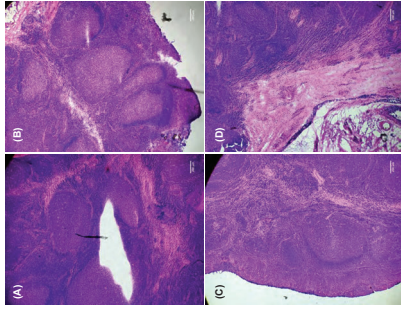
### Cell Death Results

Representative H&E images to the right:

- A: (-)**BPD** (-)**Laser**
- B: (+)**BPD** (-)**Laser**
- C: (-)**BPD** (+)**Laser**
- D: (+)**BPD** (+)**Laser**

Necrotic pattern is characterized by light pink staining with sparse nuclei - this is evident in all groups due to inherent death of excised tissue.

Qualitatively, most widespread necrotic area observed in (+)**BPD**(+)**Laser**, suggesting effective induction of cell death with full treatment.



## Conclusions & Future Work

Through our capstone project we have illustrated a possible application for PDT as an alternative to tonsillectomies that has not previously been explored. Our preliminary research suggests that L-BPD is capable of penetrating excised tonsil tissue and, in combination with irradiation, induces cell death. Further work needs to be done to validate the procedure before introducing it to the clinical setting:

1. More precise quantification of cell death to establish efficacy of PDT for removal of tonsil tissue
1. Animal studies to fully characterize the ability of the procedure to remove tonsil tissue and possibly provide insight regarding pain and safety

## Ethical Considerations

Application of this procedure would positively impact physicians, patients, and patient families. Patients and families would benefit from decreased pain, recovery time, and risk of hemorrhage. The decreased recovery time and need for return visits would allow physicians to focus on other cases. However, perception of utilizing lasers in a child's procedure carries some stigma, which would have to be mitigated.

## Significant References

1. Voth M, Wang Z, Prokhorov M, Hermit D, Higrans B, Shapovalov S. Mucosal/intra-cavitary laser tonillar ablation. *Arch Otolaryngol Head Neck Surg.* 1996;123(12):1355-1359.
2. Call JP, Spring BD, Bovi L, et al. Imaging and photodynamic therapy: mechanisms, monitoring, and optimization. *Chem Rev.* 2010;110(15):7295-2838.

## **Photodynamic Therapy as an Alternative to Tonsillectomy Procedures**

Justin Sylvers, Arley Wolfand, N. Zachary Rausch, Natalia Ochman, and Jason Chiang

A tonsillectomy is one of the most common surgical procedures in the United States, with more than 530,000 performed annually as of 2011. In this procedure tonsils are removed due to recurrent inflammation, sleep disorders, or complications from being enlarged. The procedure can be performed by different modes of excision such as cold knife surgery and electrocautery; however, complications of all tonsillectomies include primary and secondary hemorrhages, infections, and a long recovery. The goal of this project was to validate an alternative procedure for tonsil removal using photodynamic therapy (PDT). The envisioned procedure involves topical application of a photosensitizing drug (PS) to the tonsil followed by a wait interval allowing the drug to localize. After this, the tonsil is to be irradiated with a low-powered diode laser causing the excitation of the PS, generation of cytotoxic species, and cell death. If the PS can localize in and destroy germinal centers of the tonsil, the tonsils should postoperatively shrink away after several weeks without cutting and the associated bleeding of standard excision.

The specific aims of the work conducted for this project were to 1) characterize the penetration of liposomal benzoporphyrin derivative (L-BPD), an FDA approved PS, into excised tonsil tissue after topical application in solution, and 2) characterize the ability of irradiation following L-BPD application to cause cell death in excised tonsil tissue. To this end, both penetration and cell death studies were performed. For the drug penetration studies, fluorescence microscopy was used to measure penetration after application of L-BPD in varying concentrations and with varying wait intervals. The greatest penetration was observed with 70  $\mu\text{M}$  L-BPD and a 30-minute incubation. For cell death studies, tonsil portions were treated with L-BPD, irradiation, both, or neither. While evidence of necrosis was visible in all groups, it was qualitatively most pronounced in the groups that had both the drug and laser applied. These results suggest that L-BPD is capable of penetrating excised tonsil tissue and, in combination with irradiation, induces cell death. This project is a promising preliminary step toward validating PDT for tonsil removal; however, further work needs to be done to validate the procedure.





A. JAMES CLARK  
SCHOOL OF ENGINEERING

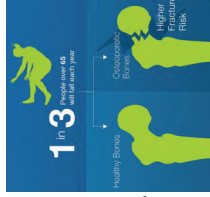
# Orthopedic Surgical Training Model for AGN1 Local Osteo-Enhancement Procedure (LOEP)

Navid Chowdhury, Daniel Lambert, Jingoe Lei, Rhea Puthumana, Josephine Stair  
Clinical Mentor: Dr. Jonathan Shaul, AgNovos Healthcare  
Faculty Advisor: Dr. Angela Jones, Fischell Department of Bioengineering, University of Maryland



## Introduction

- ❖ **Background:**
- ❖ Approximately 200 million women are affected by osteoporosis, a metabolic disease in which the bone material becomes porous and fragile.
- ❖ Nearly 1.6 million of osteoporotic patients suffer from hip fractures leading to 50% rate of depression and loss of mobility.<sup>1</sup>



### Agnovos' Solution:

- ❖ The AGN1 synthetic biomaterial is used to replace and restore functionality to the diseased bone.
- ❖ In the local osteo-enhancement procedure (LOEP), AGN1 is injected into the femoral head of the patient, where it hardens to reduce the fragility of the bone and increase bone density.<sup>2</sup>



Figure 1. Injection of AGN1 into the femur head of an osteoporotic patient during LOEP.

### Problems of Current Surgical Model in the Market:

- ❖ Expensive (approximately \$70 per model)
- ❖ Difficult to stabilize in fixed position during procedure
- ❖ Not watertight (cannot recreate LOEP irrigation and suction steps)
- ❖ Not reusable

## Objectives

- ❖ To design and create a surgical training model that is cost-efficient, easy to use, and reusable to simulate the LOEP procedure

## Ethical Implications

- ❖ Our training model must ensure user proficiency for orthopedic surgeons so that they can provide the best care for their patients
- ❖ Our training model must accurately imitate real cadaver conditions in order to prevent medical complications during real-time procedures

### References:

1. Facts and Statistics. (2017). Retrieved from <https://www.iofbonehealth.org/facts-statistics>
2. Shaul, J., et al. (2017). Resorbable AGN1 Biomaterial Centers Biomechanical Integrity to Osteoporotic Cadaveric Femurs. Retrieved from <http://www.ors.org/Transactions/63/1342.pdf>

## Design Concept

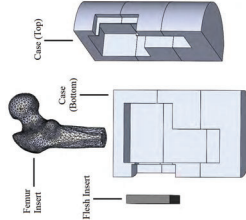
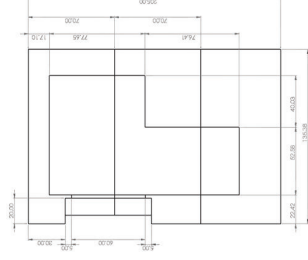


Figure 2. The three components of our model. The case is reused for multiple training sessions and the femur head and flesh insert are replaced with each use. The case dimensions are provided on the right.



## Results

### Materials Testing:

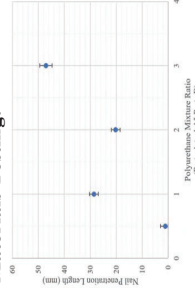


Figure 3. Foam nail-weight impact test results. Increasing the ratio of A to B when mixing the polyurethane foam solutions yielded more brittle foam results. Having less than the recommended 1:1.15 ratio yielded foam that was too spongy and deformed easily. Triplicate samples analyzed for each ratio.

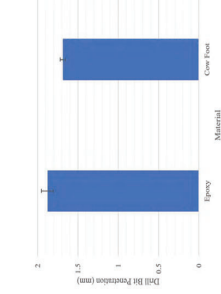


Figure 4. Epoxy timed drill penetration test results for t = 10s. The epoxy was determined to be an acceptable representation for the trabecular layer of bone, as the drill bit penetrated a similar distance in both sets of trials. Triplicate samples analyzed for each ratio.

### LOEP Tutorial App Design:

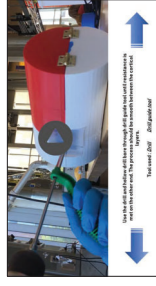


Figure 5. The computation application features a stepwise video demonstration and descriptions of steps, with links to the tools used in each step.

### Cost Analysis:

Item	Item Part Unit	Item Cost
3D Printed Log Case	1	\$50.55
Hinges (Case In)	2	\$2.65
Silicone rubber (Skin)	1	\$4.17
Humintic Medical Gel (Muscle)	1	\$6.00
Epoxy Resin Coating (Outer Bone)	1	\$4.37
Polyurethane Foam (Inner Bone)	1	\$0.53
Padding (Bone)	1	\$0.20
<b>Total</b>		<b>\$65.42</b>

Table 1. Aside from the skin, muscle, outer bone, and inner bone components, all other parts are reusable. Thus, the total cost of a model after the initial production cost would be \$12.07.

## Methods

### Prototype Development:



Figure 6. (a) Silicone rubber mold developed using an anatomical femur bone model. (b) Polyurethane foam used to create inner bone for femur model using the optimal 2:1 (A:B) ratio. (c) Epoxy resin applied to polyurethane foam for outer bone coating.

### Testing Methods:



Figure 7. (a) Polyurethane foam ratio testing for inner bone composition of osteoporotic patients. (b) Cow bone used for inner and outer bone comparison testing. (c) Drill test conducted on epoxy resin coating for outer bone composition of osteoporotic patients.

## Future Work

- ❖ Expand surgical applications of training model to other bone-related procedures such as hip replacement surgery
- ❖ Expand tutorial app to monitor time taken to complete procedure

## Conclusions

### Model Performance:

- ❖ Our training model meets the requirement of being low-cost: the \$12.07 cost of our bone and muscle insert is much lower than the \$60 figure associated with the custom Sawbones model.
- ❖ The app provides an intuitive walk-through of the training procedure, and the case allows the bone and flesh inserts to be replaced easily.
- ❖ Trainees are able to carry out the irrigation step of the LOEP procedure using our waterproof femur head.

## **Orthopedic Surgical Training Model for AGN1 Local Osteo-Enhancement Procedure (LOEP)**

Navid Chowdhury, Daniel Lambert, Jingce Lei, Rhea Puthumana, Josephine Stair

Osteoporosis is a metabolic disease that reduces the density and quality of bone. As the bone becomes more porous and fragile, there is an increased chance that a fracture may occur. Agnovos has developed a new synthetic biomaterial called AGN1 to replace and restore functionality to osteoporotic bone. In the local osteo-enhancement procedure (LOEP), AGN1 is injected into the femoral head of the patient. Currently, Agnovos employs a customized femur model made by Sawbones as a training model for simulation and training. The purpose of this project is to create an alternative training model for the LOEP surgery that is cheaper, more realistic, and more practical to use. Our model has three principle components: a reusable outer case, disposable femur head and flesh inserts, and a tutorial application. The 3D-printed outer case simulates the upper thigh and holds the bone model in place. The femur head was created by setting polyurethane foam in a silicon mold and coating the shaped foam in epoxy resin. The optimal mixing ratio of the polyurethane foam was determined through a nail-weight impact test. The flesh insert is comprised of Humimic Medical Gel and a thin layer of silicon, simulating muscle and skin, respectively. The application provides an intuitive walk-through of the training procedure using our model. We met our goal of developing a cheaper alternative to the \$70 Sawbones model. The total one-time cost of our case was \$53.35, and the cost for a set of disposable femur head and muscle inserts is \$12.07. Our femur model is watertight, allowing trainees to perform the irrigation and aspiration steps of the LOEP procedure, and the case itself allows the bone to be easily inserted and replaced during training. Overall, we have created a suitable alternative to the currently-used Sawbones model that is cheaper, more realistic, and easier to use.

# PID Controlled Hemofiltration for Poison Control

Vaidehi Bhagat<sup>1</sup>, James Bookhultz<sup>2</sup>, Elliot Bromberg<sup>3</sup>, Akshaya Ganesh<sup>4</sup>, Chris Kuffner<sup>5</sup>  
 Advisors: Dr. Alison Grazioli, Dr. Josh King, Dr. Zhongjun Wu, University of Maryland Medical Center

## Objective

The Maryland Poison Control center handles about 44,000 calls a year regarding people who have been poisoned with substances such as household chemicals, alcohol or opioids, that cannot be easily cleared using current hemofiltration methods. This project aims to improve hemofiltration by utilizing the power of ECMO. In order to accomplish this, the pump must meet the demands of ECMO and hemofiltration while and manage a flow rate of up to 5 Liters per minute (Lpm) through the main pump. The selected design involved programming a microcontroller to adjust the rate at which a roller pump pumps the effluent fluid from the filter based upon the measured flow rates. The device must be durable, capable of running for days, portable, and not too expensive.

## Methods

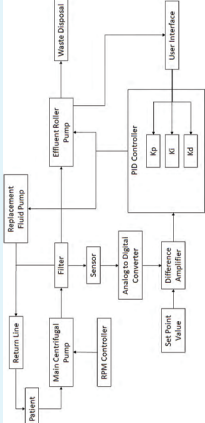


Figure 1. Schematic of set in which the flow sensor is used as an input for the PID controller which feeds a voltage and drives the effluent and replacement roller pumps.

An Arduino Uno will be used to create a PID controller for a pump. The hemocompatible pump was provided by Dr. Wu and has access to required ports for motor speed control. The sensor used to measure the flow rate for the PID controller is an ultrasonic flow sensor that can also be used with blood, allowing the designed system to run with blood. The system design allows it to be compatible with any filter design the cooperating team develops. A circuit will be needed to amplify the current produced by the Arduino since it is only capable of producing low currents that cannot drive a motor. The motor to be controlled in this diagram is the effluent pump which will see less flow than 5 Lpm. The pump being controlled can only achieve a flow rate of around 3 Lpm which should serve our needs.

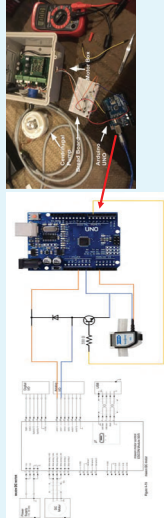


Figure 2. Depiction of connections between the Arduino board and flow rate control system.



Figure 3. Full hemofiltration system set up with 8 filters in parallel (made by filter team with circuit setup of the motorbox)

The pump control system was created using the AutoPID tool box in Arduino along with a small circuit portion to allow the output of the Arduino controller to be amplified to a higher current than the output pins are capable of. The pump control system went through many iterations before it was entirely ready to be put into use. The original setup reached the setpoint after about three minutes of running. This was because the inputs in the PID equation were too low, resulting in a very slowly changing output. The issue was fixed by multiplying the setpoint and voltage read from the sensor by the same value. This amplified the output of the PID controller, and did not interfere with reaching the setpoint. A second version of the code was created to allow for monitoring the flow rate and run time from a computer using Arduinos serial plotter. The Arduino fed the output of the PID into a controller for the motor that is provided by Maxon Motors for this specific motor and contains a 120V power supply and motor winding and controls as well as inputs for external commands.

## Results

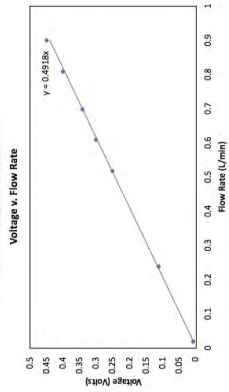


Figure 4. Flow rate vs the read voltage

A relation between the voltage output from the sensor to the read flow rate was established by generating a trend line through various recorded points. The relation was found to be approximately 0.1V for every 0.2 Lpm of flow. This relationship was needed to convert the desired setpoint to a voltage that could be compared to the voltage being read by the flow sensor. The code feeds a PWM signal to the motor control box that can be used to increase the flow as needed based upon what is read from the sensor.

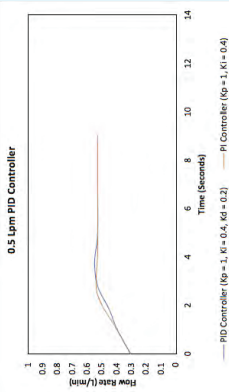


Figure 5. Change in flow rate over time using PI control at 0.5 Lpm

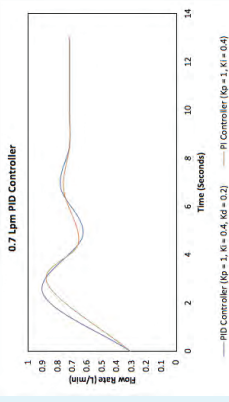


Figure 6. Change in flow rate over time using PI control at 0.7 Lpm

It was found that the PI controller was favorable in both cases of flow rates. The PI controller resulted in less overshooting and a faster response in the case of the 0.5 Lpm trial. The controller was observed to cause more overshooting at higher flow rates. More combinations of controller setting could be tested later on to lessen overshooting. The trials were done with a lower flow rate than intended in the actual design in capable of being scaled up to accommodate a flow of 5 Lpm through the main pump and up to 3 Lpm through the effluent pump.

## Ethical Implications

Hemofiltration using the technology of traditional ECMO to filter blood at rates higher than currently possible, is novel, but poses minimal threat to the public. The technology is already available and widely accepted in the medical community. Potential risks of the system include air entrapment in the circuit, blood loss, and hemodynamic instability in case of device malfunction and must be addressed when advancing the design for clinical use.

## Conclusions

A feedback controller was built to maintain consistent flow rates for hemofiltration and similar applications. The controller can respond to changing conditions and maintains its function across multiple hemofiltration systems. One of the systems tested involved parallel filters engineered by another capstone team, so this controller may be especially useful when implementing novel hemofiltration devices. Its sensing function enables instant, automated tuning when, normally, a medical professional would have to manually adjust settings. This may be of great value for the other team's parallel filter mechanism, which was designed in part to treat drug overdoses. It will be critical in such unpredictable situations where time is of the essence.

## Future Work

In the future the system should be tested in actual blood or a blood mimetic since tests with the controller were only done on saline solutions and water. The results of this test can be used to further determine how the system will interact in a hospital setting on a patient. Finally, a user interface could be added to the controller to create a system that is easier to manipulate. This would also allow for plotting of the flow rates at each point in the system for easy analysis of the performance of the controller.

## References

- Downing, R. (2017). AutoPID. Retrieved from <https://r-downing.github.io/AutoPID/>
- Ghannoum, M., Hofmann, R. S., Gosselin, S., Nolin, T. D., Lavergne, V., & Roberts, D. M. (2018). Use of extracorporeal treatments in the management of poisonings. *Kidney International*, 94(4), 682-688. doi:10.1016/j.kint.2018.03.026
- Maxon Motor. (2018). ESCON Module 50/5 Servo Controller: Hardware Reference. Sachseln, Switzerland: Maxon Motor.

Acknowledgements: A special thanks to our Capstone professors Dr. Tao and Dr. Lan Ma as well as our mentors Dr. Grazioli, Dr. King, and Dr. Wu for their continuous support.

## **PID Controlled Hemofiltration for Poison Control**

Vaidehi Bhagat, James Bookhultz, Elliot Bromberg, Akshaya Ganesh, Chris Kuffner

According to the U.S. Renal Data System Annual Report, there are currently over 660,000 Americans being treated for kidney failure and 468,000 of those patients are on dialysis. The kidney has several functions, including filtering blood and the excretion of wastes and toxins from the body. When a patient has renal failure they often undergo dialysis, a process in which the patient is attached to a machine which performs the filtering functions of the kidney, mechanically. Although dialysis is typically used for patients undergoing chronic renal failure, and often doesn't handle sufficient enough blood volumes to treat acute renal failure. The Maryland Poison Control center handles about 44,000 calls a year regarding people who have been poisoned with substances such as household chemicals, snake venom, alcohol or opioids.

Hemofiltration will be used to treat patients suffering from acute renal failure rather than traditional dialysis. High hemofiltration clearance levels can be achieved by taking advantage of Extracorporeal Membrane Oxygenation (ECMO). ECMO technology is capable of oxygenating the body's blood volume at a rate of 5L/min. By applying this technology to hemofiltration, thousands of lives could be saved.

Proportional Integral Derivative (PID) control was implemented using an Arduino microcontroller in order to set the flow rate for fluid replacement equivalent to the flow rate of effluent being filtered out from the system once the saline solution from the main centrifugal pump was filtered. The user could set the flow rate at which the effluent was being filtered out and the system would correct the flow rate to that value.

Results of the testing conducted showed that the relationship between Lpm and read voltage was approximately 0.1V for every 0.2 Lpm of flow. This relationship was needed to convert the desired setpoint to a voltage that could be compared to the voltage being read by the flow sensor. Based off of the information received by the sensor, the controller can adjust the flow rate as necessary. The PID controller was tested at two different flow rates against a PI controller to determine which overshoot less at the two flow rates. It was found that the PI controller was favorable in both cases of flow rates. The PI controller resulted in less overshooting and a faster response in the case of the 0.5 Lpm trial. The controller was observed to cause more overshooting at higher flow rates. This device will improve outcomes for patients with acute renal failure cases that could not be treated using current methods.

# Scapholunate Ligament Augmentation System for Rapid Functional Restoration

Alec Boyle, Chris Damiani, McKenzie Figur, and Adriana Meriles-Medina

Advisors: Dr. R. Frank Henn III, University of Maryland School of Medicine / Dr. K Herold, Fischell Department of Bioengineering, University of Maryland

## Clinical Need

### Objective

Devise a novel ligament augmentation device applicable to complete tears of the scapholunate ligament (SLL) with or without scaphoid and lunate malalignment. This device will allow flexibility and range of motion during the healing process while providing a secure connection between the scaphoid and the lunate able to withstand normal tensile loads.

- Scapholunate Ligament (SLL) is primary stabilizer of the wrist
  - Cup shape ligament composed of 3 sections
  - Flexion and radial-ulnar deviation
- Stage 2, 3, and 4 Scapholunate Dissociation (SLD): Complete rupture of SLL with intact cartilage.
  - Stages 2 and 3: aligned scaphoid and lunate
  - Stage 4: malaligned scaphoid and lunate [3].
- Improper healing can result in:
  - Reduced range of motion and weakness
  - Long term osteoarthritis
  - Scapholunate advanced collapse (SLAC)

### Motivation: Inadequate Surgical Solutions

- Multitude of current surgical repair procedures
- Current procedures have inadequate long term results
  - Pinning → reduced range of motion and flexibility
  - Suturing → inadequate strength
  - Rate of re-rupture high after surgical repair
  - Inability to return to peak performance

## Device Design

After surgical repair of the scapholunate ligament in stage 2 SLD, our intraosseous device will be placed to augment the weakened ligament, allowing for optimal healing. For stage 3 and 4 SLD, the irreparable ligament will be replaced by our device. The device will be secured internally into both the scaphoid and the lunate, and the polyethylene sutures will hold these internal connections in tension to bear wrist loading.

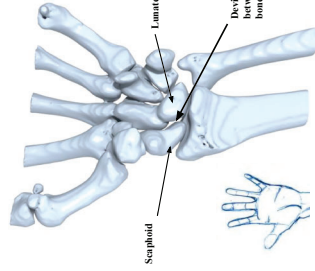


Figure 2: Anatomy of a patient's left hand shown palm out. CAD model developed based on an anonymous CT scan provided by our clinical mentor

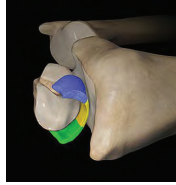


Figure 1: Cross section of SLL. Distal (blue), Proximal (yellow), Volar (green)



Figure 3: Solidworks render of our device, consisting of a polypropylene spacer, a tapered peak headless screw, and polyethylene suture wires

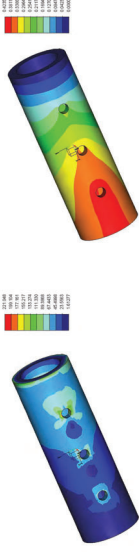
### 3 Key Design Features

- Strength:** Able to bear as much tensile load as the SL ligament (260N) [4].
- Flexibility:** Allow rehabilitation exercises to begin within 2 weeks of surgery.
- Bone Health:** Small device for minimal drilling of bone, as drilling may cause bone weakness or osteonecrosis in rare cases [6].

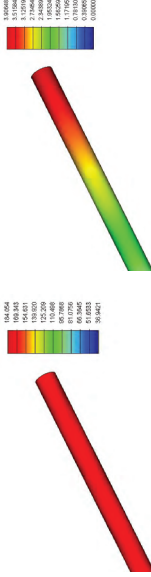
## Mechanical Testing

### Finite Element Analysis

Model device simulated in tension at the maximum required force capabilities of an intact Scapholunate Ligament, 260 N [4].



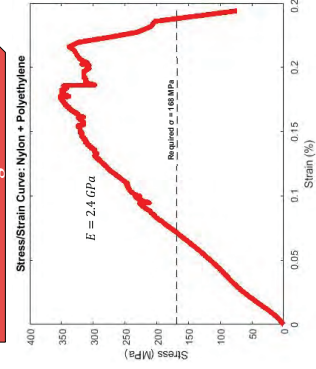
**Max Stress:** 221 MPa  
Polypropylene spacers show high stress-bearing capabilities and low displacement. Polyethylene suture will be limiting factor for stress and displacement.



**Max Stress:** 184 MPa  
Polyethylene spans between scaphoid and lunate 4 times in our device, increasing the effective cross sectional area of the sutures by a factor of 4.

To model this for stress testing, cross sectional area in model is multiplied by 4

### Tensile Testing



Device tested under tensile loads until failure. Peak stress was 352 MPa (524 N), well above the required 168 MPa (260 N).

Stress-strain curve and Young's Modulus are characteristic of Polyethylene

$$\sigma_{Req} = \frac{260 \text{ N}}{4 \times [\pi \times 0.00035]^2} = 168 \text{ MPa}$$

$$FOS = \frac{352 \text{ MPa}}{168 \text{ MPa}} = 2.1$$

$$F_{Fail} = 542 \text{ N} = 352 \text{ MPa}$$

$$F_{Allow} = 260 \text{ N} = 168 \text{ MPa}$$

## Conclusion

Our clinical mentor provided us with a unique challenge: combining strength and flexibility in our device. Using the engineering design process we were able to implement a feasible and reproducible solution which met both of these requirements

### Conclusions

- Elimination of pinning, increased flexibility
- Ability to withstand expected loading of 260 N with a safety factor of 2.1
- We learned:
  - Access to medical-grade, sterile materials and cadaver specimens provides a significant barrier to entry in the field of medical device design
  - The process of innovating medical technologies can be extensive and time consuming, but in the end it is rewarding
  - Identifying a need, generating a concept, developing strategies and planning, and integrating the parts of the new device require teamwork and dedication
- Ethical Implications**
  - Surgeons must learn new surgical procedure
  - Higher level of confidence in athletes returning to preinjury level of competition
  - Expensive procedure, patients unable to afford surgery can be subject to increased progressive arthritis and wrist pain
  - Invasive surgery is associated with increased risk to patients such infection and osteonecrosis in rare cases

## Future Work

### Additional Testing

- Perform in vitro force analysis tests with cadavers for accurate mechanical model
- Conduct animal in vivo studies to study host immunological response and other potential risks associated with materials or design of the device
- Analysis of stress-strain curve for anatomically sized model
- Insert device into cadaver hand model with appropriate surgical tools

### Design Modifications

- Completely bioresorbable design to address stage 2 SLD
- Revise the cylinder design to an expandable sheath to facilitate insertion, similar to existing screw-in-sheath constructs used in ACL reconstruction such as IntraFix®

### FDA Approval

- FDA approval once appropriate test in animal models and cadavers are performed to determine that device is at least as safe and effective as other available devices [5]
- Submit Premarket Notification 510 (K)

## Acknowledgements

We extend our gratitude to Dr. R. Frank Henn III for his guidance and extensive orthopedic knowledge. Additionally, we thank Dr. Keith Herold for advising us throughout the duration of this project and serving as our faculty advisor. Special thanks to Dr. Zhongjun for a steat donation and to Mike Gaczyński for his assistance in mechanical testing. Lastly, we thank the Fischell Department of Bioengineering for this opportunity to explore an area of interest and the resources to succeed in this capstone.

## References

- Background image: <http://allhandbooks.com/wp-content/uploads/2016/05/14-Wrist-Diagram.jpg>
- Motion from: <http://www.youtube.com/watch?v=Ugk38p3t300>
- Cartilage: <https://www.youtube.com/watch?v=Ugk38p3t300>
- Cartilage: <https://www.youtube.com/watch?v=Ugk38p3t300>
- U.S. Food & Drug Administration. Premarket Notification 510 (K). <http://www.fda.gov/medical-devices/premarket-notifications/premarket-notification-510k>
- Parkley, E. K., & Prada, S. S. (2013, March 4). Drilling of Bone: A comprehensive review. Retrieved from <http://www.ncbi.nlm.nih.gov/pmc/articles/PMC3801511/>

## **Scapholunate Ligament Augmentation System for Rapid Functional Restoration**

Alec Boyle, Chris Damiani, McKenzie Figur, and Adriana Meriles-Medina

The scapholunate ligament serves a critical role in stabilizing the wrist and providing support during physical activities. However, its prominent role and complexity within the carpal system make ruptures of the scapholunate ligament (SLL) one of the most common and complicated types of wrist injuries. Multitudes of methods exist to surgically repair the system to regain functionality, but these methods are inadequate, and many have long-term side effects such as high re-tear rates, reduced range of motion and flexibility, and an inability for the patient to return to peak performance. The current procedures are highly dependent on the stage of the scapholunate dissociation (SLD). The six stages are categorized by quantifying the degree of tear (complete or partial), the possibility of repair of the ligament, alignment or malalignment of the scaphoid, and cartilage health. Our device will be applicable to complete tears of the ligament with and without malalignment of the scaphoid, which correspond to stages 2 through 4. Our team proposed to work towards solving this medical problem with applications of mechanics and surgical engineering principles. Under the guidance of our clinical mentor, Dr. R. Frank Henn III, an orthopedic surgeon at the University Of Maryland School Of Medicine, we designed a reliable method for surgically augmenting the ruptured scapholunate ligament to restore functional mobility without sacrificing long-term stability. Our intent was to establish a method of repair that is common across orthopedic practices and replaces the multitude of less desirable methods used today. The purpose of our device is to augment the scapholunate ligament as it heals for stage 2 SLD or to replace the native ligament for stages 3 and 4 SLD. Our design consists of two spacers made of polypropylene that can be inserted into the scaphoid and lunate. Much like drywall anchors, these spacers expand with the insertion of polyether ether ketone (PEEK) screws and are held in tension with polyethylene suture. The maximum force the native SLL ligament can withstand is 260 N. Both FEA simulations and mechanical testing have shown our device is capable of holding far greater loads than required, with a safety factor above 2. Our device provides the load-bearing capabilities to effectively hold the scaphoid and lunate in tension while providing the flexibility necessary to return to functional movement quickly.



# Vesicular Delivery of Interleukin-11 gene for osteoporosis treatment

Elizabeth Bentley, Corinne Farley, Matt Mulvaney, Maria Pozo, Eric Wang  
Faculty Advisor: Dr. Steven Jay, Fischell Department of Bioengineering, University of Maryland  
Clinical Mentor: Dr. Stephen Thom, Department of Emergency Medicine, University of Maryland Baltimore



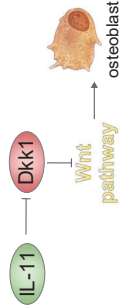
## Background

### Osteoporosis

- Over 200M people with osteoporosis
- Decreased quality of life

### Critical Pathway

- Wnt signaling promotes osteoblastogenesis
- Proteins Dkk1 and Dkk2 are Wnt inhibitors
- Interleukin-11 (IL-11) inhibits Dkk1 and Dkk2



### Extracellular Vesicles as Drug Delivery System

- Bodies that bud off of cell membranes
- Self-origin mitigates immunogenicity
- Surfaces can be conjugated for targeting

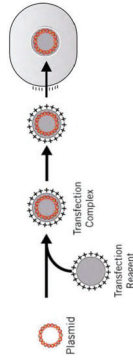


### Our Solution

- Engineer plasmid containing *IL-11* gene
- Load plasmid into extracellular vesicles (EVs)
- Introduce EVs to bone area to promote osteoblastogenesis

## Methods

### Adapted Transfection: Plasmid into EVs



### Loading Quantification

- Lyse EVs
- Measure genetic content using Nanodrop spectrophotometer

### Introduction to Human Embryonic Kidney Cells

- HEK293T incubated with model GFP plasmid-loaded EVs

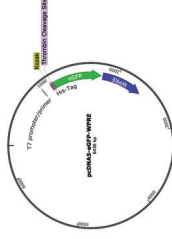
### Expression Quantification

- Microplate photometer measures expression of GFP

## Results

### What We Did

- Loaded model plasmid pcDNA5-eGFP into EVs
- Introduced loaded EVs to HEK293T cells to determine viability as delivery system



### Loading Efficiency

Initial Input  $\left\{ \begin{array}{l} 40 \mu\text{L of } 167.2 \mu\text{L used for quantification} \\ 1500 \text{ ng of pcDNA5-eGFP loaded} \\ \frac{40 \mu\text{L}}{167.2 \mu\text{L}} \cdot 1500 \text{ ng plasmid} = 360 \text{ ng loaded} \end{array} \right.$

Loaded  $\left\{ \begin{array}{l} \text{Nanodrop yielded } 6.1 \text{ ng}/\mu\text{L concentration} \\ 15 \mu\text{L suspension after miniprep} \\ 6.1 \frac{\text{ng}}{\mu\text{L}} \cdot 15 \mu\text{L} = 91.5 \text{ ng} \\ \frac{91.5 \text{ ng}}{360 \text{ ng}} = 0.254 \\ \therefore 25.4\% \text{ loading efficiency} \end{array} \right.$

### Fluorescence Data

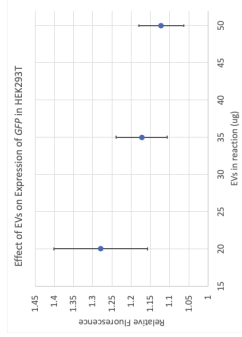


Figure 1. Plate reader results when 20, 35, and 50  $\mu\text{g}$  of pcDNA5-eGFP loaded EVs are incubated with HEK293T cells overnight. Error bars represent std. dev. between duplicates. Data normalized to 1 (divided by neg. control).

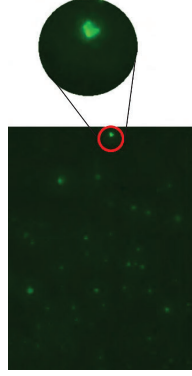


Figure 2. Microscopy image of HEK293T cells incubated with 20  $\mu\text{g}$  of pcDNA5-eGFP loaded EVs.

## Ethics

### Experimental Ethics

- Animal testing
- Isolation procedures: human subjects

### Application Ethics

- Other uses for osteoblastogenesis
- Athletics



## Conclusions

- Transferring GFP into EVs results in ~25.4% loading efficiency
- Incubation with HEK293T cells produces GFP expression
- Method can be extended to *IL-11* expression to treat osteoporosis

## Impact and Future Work

### Benefits of the Device

- Personalized medical treatment
- Non-invasive approach
- Platform can be modified for wide range of applications

### Future Work

- Design *IL-11* encoding plasmid
- Use of (AspSer)<sub>6</sub> to target bone-formation surfaces
- *In Vivo* animal models
- Downstream processing for purification
- Scale-up for high throughput production

## Acknowledgements

This work was supported by the Capstone program in the Fischell Department of Bioengineering at the University of Maryland. Mentorship was provided by Dr. Steven Jay (University of Maryland, College Park) and Dr. Stephen Thom (University of Maryland, Baltimore). Lab space and materials were provided by Dr. Jay's lab, and initial vesicle samples were provided by Dr. Thom's lab.

## References

Lamichhane, T. N., Jay, S. M., Production of Extracellular Vesicles Loaded with Therapeutic Cargo. *Methods Mol Biol* 2018, 1713, 171-187.

Rutkowski, A.; Sienkiewicz, K.-O.; Vaseg, J. J., Osteoblast Differentiation at a Glance. *Medical Science Monitor Basic Research* 2016, 22, 95-106.

Sozen, T.; Ozsik, L.; Basaran, N. C., An overview and management of osteoporosis. *Eur J Rheumatol* 2017, 4 (1), 46-56.

Zhang, G.; Guo, B.; Wu, H.; Tang, T.; Zhang, B.; Zheng, L.; ... Qin, L. (2012). A delivery system targeting bone formation surfaces to facilitate RNA-based anabolic therapy. *Nature Medicine*, 18(2), 307-314. doi:10.1038/nm.2617

## **Vesicular Delivery of Interleukin-11 gene for osteoporosis treatment**

Elizabeth Bentley, Corinne Farley, Matt Mulvaney, Maria Pozo, Eric Wang

Osteoporosis is a disease characterized by a reduction in bone density, resulting from an imbalance in the rates of bone deposition and bone resorption. Current treatments for osteoporosis include various medications, such as hormone-related therapy, that often put the individual at risk for blood clots, heart disease and several cancers. To address these challenges, gene therapy utilizing extracellular vesicles (EVs) could be used to promote osteoblastogenesis. Due to their self-origin, flexibility, and ability for surface conjugation, EVs mitigate immunogenicity and systemic clearance of other drug delivery systems. Here, we “transfect” EVs with plasmid DNA and carry genetic content to target cells, facilitating gene expression. Specifically, we delivered a model fluorescence plasmid to human embryonic kidney cells and saw observable expression of GFP. Our results indicate the feasibility of patient-derived EVs as personalized plasmid delivery systems.



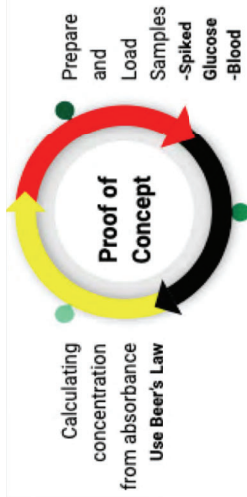
# In-Line Blood Analyzer For Premature Infants

Sarah Asfari, James Fookes, Adam Herskovits, Devon Parsons, Cristina Tous  
Advisor(s): Dr. Silvina Matysiak, The Fischell Department of Bioengineering, University of Maryland / Dr. Sripriya Sundararajan, MD, UMD School of Medicine

## Motivation/Objective

Blood analyte levels of premature babies need to be continuously monitored, but lowered blood levels can cause more stress on babies leading to life-threatening shock. A very low birth weight infant has a very small circulating blood volume, typically having only 80-100ml /kg, and they can lose large volumes of blood to laboratory testing in the first few weeks of their life<sup>1</sup>. The current methods require about 5 ml of blood to be taken for each test, and numerous tests can be conducted in a given day<sup>2</sup>. New devices have been created to reduce the amount of blood that is needed for each test, but this still introduces the risks associated with taking a blood from such a small infant. We aim to create a device that can measure the blood analytes in premature babies without the need to remove blood from them.

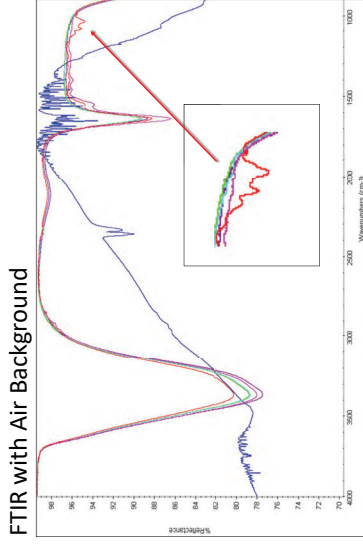
## Methods



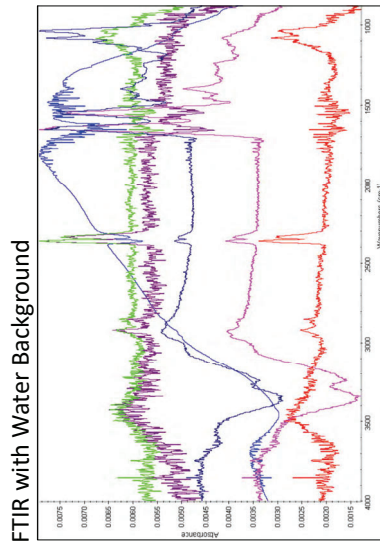
## Ethical Implications

Our project strives to reduce blood withdrawal from neonates which will reduce the amount of stress placed on a premature infant's aerobic system. We additionally want to reduce the amount of blood transfusions which will reduce the chance of the baby going into life threatening shock. This will improve the premature baby's chance at living a normal, healthy life in the future.

## Results



- Air Background
- Water
- 20mM Glucose Solution
- 50mM Glucose Solution
- Bovine Blood
- Bovine Blood + Glucose



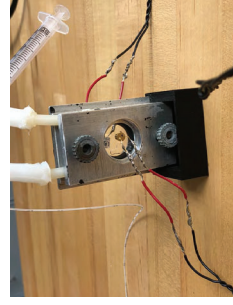
- Water Background
- Water
- 20mM Glucose Solution
- 50mM Glucose Solution
- Bovine Blood
- Bovine Blood + Glucose

From the graphs obtained using the FTIR machine, a difference in peak intensity can be observed between the samples. Not much can be determined from the air background graph, other than that blood and glucose share similar peaks. Glucose can be seen in peaks present at wavenumbers of 1012 and 1081 in the figures above, which are known values for glucose peaks<sup>3</sup>. On the water background graph, both the regular blood and blood+ 4 wt% glucose have peaks that are higher than that of water but lower than the pure glucose solutions<sup>3</sup>.

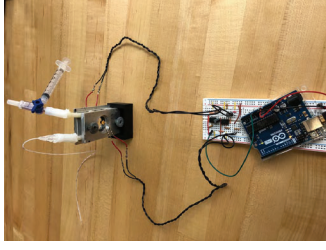
Concentration of glucose can be determined using Beer's Law. The equation  $A = \epsilon \cdot c \cdot l$ , the molar extinction coefficient for glucose can be determined, given that A, l, and c are known values. From experimental data, it was determined empirically that  $\epsilon$  is roughly 0.023. This means that, given the measure absorbance of an unknown sample of glucose solution, concentration can be calculated using  $C = A / (l * \epsilon)$ .

## Conclusions

- Proof of concept demonstrated using Infrared light sensor instead of FTIR system due to cost restraints
- In-line analyzer was designed with Arduino, infrared sensor, infrared light source, and specialized flow through cuvette
- Blood samples were loaded by applying a suction using an inline syringe to eliminate blood loss
- Concentration of analytes calculated using Beer's Law with measured absorbance values



Internal components of device without the outer housing. Image on the left is the flow-through cuvette and sensors. Image on the right is the general set up.



## Future Work

Given more time and a larger budget, this project could be furthered by:

- Replacing the infrared sensor with an FTIR sensor, which would enable the ability to detect all desired analytes
- Calibration testing to increase precision and accuracy of concentration calculations
- Improving accuracy of detection, and focusing the range of detection to target specific analytes while filtering out most of the background

## Significant References

1. Vincent, J. L. et al. Anemia and blood transfusion in critically ill patients. *Jama* 288, 1499-1507 (2002).
2. The blood volume of infants. *Stoner, Thomas R.C. et al. The Journal of Pediatrics*, Volume 35, Issue 4, 439 - 446.
3. Smith, B. C. (2017). An IR Spectral Interpretation Repository: Carbohydrates and Alkynes. *Spectroscopy* 34(7). Retrieved May 5, 2019, from <http://www.spectroscopyonline.com/ir-spectral-interpretation-polymer-carbohydrates-and-alkynes>.

## **In-line Blood Analyzer for Premature Infants**

Sarah Asfari, James Fookes, Adam Herskovits, Devon Parsons, Cristina Tous

The health and development of a premature infant in the neonatal intensive care unit (NICU) is currently assessed by measuring the concentration of various analytes at any given time. The typical analytes that are measured include: lactate, oxygen saturation, glucose, urea, creatinine, sodium, potassium, magnesium, and calcium. Blood testing is currently used to determine the concentration of these analytes. These blood tests require a new 5 milliliter sample to be taken each time the concentration of an analyte is to be determined. The accumulation of these blood draws during the early postnatal period can result in the infant losing an estimated 10-20 mL of blood/kg per week, or 15%-30% of their circulating blood volume in the first weeks of life. This loss in blood volume commonly results in the premature infants becoming anemic, and also places a large amount of stress on their aerobic, skeletal, and cardiovascular systems. We eliminated the need for blood withdrawal by designing an in-line blood analyzer that determines analyte concentration using Fourier Transform Infrared Spectroscopy (FTIR). The analyzer consists of a catheter line from the premature infant attached to one input of a flow through cuvette. The other input of the cuvette contains a port for a syringe to be attached. The blood can be drawn into the cuvette by applying suction via a syringe. The flow through cuvette can then be placed into an opaque box containing the FTIR spectrophotometer, which will measure the amount of light absorbed by the blood sample. The concentration of the blood analytes are then determined by inputting the absorption values into Beer's law. The concentration of specific analytes are targeted by using absorption values of peaks at specific wavelengths that are known to be characteristic of a molecule. Once the concentration is determined, the blood can be returned back into the infant's body by pushing down on the plunger of the syringe. Due to cost restraints, an FTIR spectrometer could not be obtained. An infrared Arduino photodiode was used as a placeholder for the FTIR spectrometer to demonstrate proof of concept. The specific peaks for glucose were determined to occur at wavenumbers of 1012  $\text{cm}^{-1}$  and 1081  $\text{cm}^{-1}$ , and isolated by subtracting out the spectrums of other analytes found in blood. Additionally, the extinction coefficient to be used in Beer's law to determine the concentration of glucose was calculated to be 0.023, and the path length of  $L \cdot \text{mm} \cdot \text{mmol}$  our design was found to be 4mm. Overall, we have succeeded in designing the framework for a novel way to measure the concentration of various analytes in the blood of a premature infant that does not require them to experience any loss in blood volume. The analyzer can be improved upon to accomplish the entire objective of detecting the concentration of all analytes by installing the proper FTIR sensor, and isolating the appropriate peaks, as was done for glucose.

# Single-Stage Percutaneous Tracheostomy Device

Subhashini Arumugam<sup>1</sup>, Zon Fatima<sup>1</sup>, Daniel Najafali<sup>1</sup>, Gabriel Sanz<sup>1</sup>, and Alya Suraya<sup>1</sup>

Advisors: Joseph Rabin M.D.<sup>2</sup> and John P. Fisher PhD<sup>1</sup>

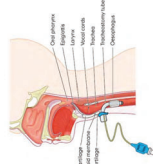
<sup>1</sup>Fischell Department of Bioengineering, A. James Clark School of Engineering, University of Maryland, USA

<sup>2</sup>University of Maryland School of Medicine, University of Maryland Baltimore, USA

## Background and Significance

### What is a Tracheostomy?

Percutaneous tracheostomy is a procedure that circumvents airway obstruction by providing an alternative route through a deliberate opening in the trachea<sup>1</sup>. It is performed at the patient's bedside, as opposed to surgical tracheostomies which are performed in the operating room. Maintaining the patient's airway allows for ventilatory support and adequate perfusion until the native airway is restored.

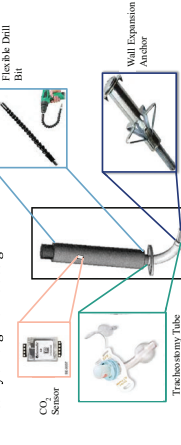


### Clinical Need

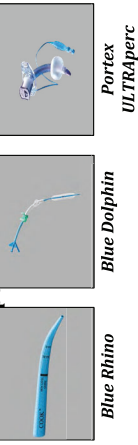
- Current methods require multiple rounds of instrumentation<sup>2</sup>:
  - Increased procedure time
  - Increased risk of infection
  - Increased risk of bleeding
- Minimal tactile feedback for the physician
- Inaccurate placement results in secondary complications<sup>3</sup>

### Objectives

- Successfully dilate an opening of the trachea to 10 millimeters in diameter
- Employ a single instrument
- Detect correct placement
- Provide tactile feedback
- Carry an ergonomic design



### Current Competitors



## Methods and Results

### Prototyping

#### Dilation Mechanism

A novel dilation mechanism is at the crux of our project, thus the first part of our prototyping process was to adapt a dilation mechanism. We tested the designs using larger-scale parts that are commercially available at hardware stores. After identifying flaws within each system, we were able to choose a wall-anchor like dilation method, and designed our components using 3D printing software. The wall anchor-like component is attached to a flexible drill bit that can be easily rotated by the physician to dilate the tracheal opening.

### 3D Printing

Our prototype design utilized a variety of printing techniques to formulate the various components, as well as an initial testing platform for our device. A rudimentary prototype was assembled with parts printed using the MakerBot 5th Generation series and Polylactic Acid filament (PLA). We identified the need for further mechanical considerations using this model, and redesigned and reprinted the parts in more various materials to better suit their intended functionality. A breakdown of key components and materials are given below:



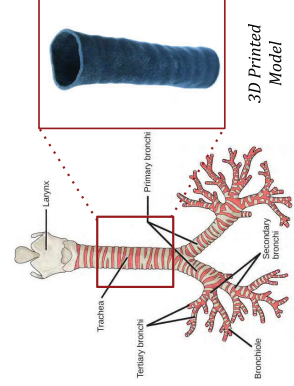
Finite Element Analysis (FEA) was conducted on three different designs for the expansion mechanism. Using these results we were able to choose the most stable design for printing and further development.

#### Maximum Stress Analysis



### Tracheal Modelling

We used CT image data to construct a 3D model of an adult trachea, printed in a combination of materials to match the elastic modulus of the cartilaginous section of the trachea (approximately 1.74 MPa). 9g of the VeroGray, 16g of the Agilus30, and 5g of the Med610 materials were used in the final model, printed on the Objet500 Connex3 printer.



## Ethical Implications

We intend to make a device that is cost-efficient and safer for patient use. In doing so we will improve accessibility, as well as patient outcomes. Initial prototyping has been conducted on 3D printed models to mitigate risk exposure of live subjects. Future analysis and studies using porcine models, and eventually patient data will require further implementation of ethical standards. Specific protocols designed with ideal conditions and proper treatment of subjects will be implemented and used with the same high ethical standards.

## Conclusions

- Developed a single stage tracheostomy tube delivery system
  - Implements a novel dilation mechanism
  - Provides continuous tactile feedback
- Investigated various material components to develop a cost-effective, easily replicable design
- Demonstrated potential to create a device with additional components to sense placement through CO<sub>2</sub> sensors as well as determine trajectory



## Future Work

We will proceed to testing our device on porcine models which are comparable to human tracheas once we have established efficacy in our 3D printed tracheal models. We then will test on cadavers to most closely replicate operating conditions before proceeding to clinical trials. Further collaboration with clinical faculty will allow us to develop a marketable and patentable design.

## Significant References

1. Rashid, A. O., & Ikem, S. (2017). Percutaneous tracheostomy: A comprehensive review. *Journal of Thoracic Disease*, 9(10), doi:10.21037/jtd.2017.09.33
2. Giunchi, et al. "Comparison between Single-Step and Balloon Dilational Tracheostomy in Intensive Care Unit—a Single-Centre, Randomized Controlled Study." *OTF Academic*, Oxford University Press, 21 Apr. 2010. academic.oup.com/otf/article/104/6/728/232461.
3. Byham, C., Wilke, H., Habbig, S., Lischie, V., & Wessphal, K. (2000). Percutaneous Dilational Tracheostomy: Capilla Blue Rhino Versus the Basic Cough Technique of Percutaneous Dilational Tracheostomy. *Anesthesia & Analgesia*, 91(3), 802-806. doi:10.1097/00000539-200010060-00021

## Acknowledgements

We would like to extend our gratitude to our mentors Dr. John Fisher, Ph.D. and Dr. Joseph Rabin, MD for their continued support throughout our project. We would also like to thank Dr. Yang Tao, Ph.D., Dr. Lan Ma, Ph.D., and the Fischell Department of Bioengineering for their efforts.

## **Single-Stage Percutaneous Tracheostomy Device**

Subhashini Arumugam, Zon Fatima, Daniel Najafali, Gabriel Sanz, Alya Suraya

A percutaneous tracheostomy is a bedside-procedure that circumvents airway obstructions and offers ventilatory support to patients via a deliberate opening in the trachea. After dilating an initial incision, a tracheostomy tube is placed in the opening to maintain airflow. Current devices used for dilation require multiple rounds of instrumentation leading to increased risk of bleeding, infection, and tracheal damage during the procedure. Further limitations in the device structure can result in a lack of passive airflow, leading to hypoxia. Thus, we propose a single-stage percutaneous tracheostomy device that further reduces this range of complications, decreases the rounds of instrumentation needed to place the tube, and improves upon tactile feedback during the procedure. A passive airflow component to address the risk of hypoxia during a tracheostomy will also be included. A prototype of our device, including a novel dilation mechanism was created using 3D printing technologies, exhibiting enhanced structural detail and cost-efficiency when compared to other methods. Considerations of the biocompatibility as well as structural integrity of our device has been investigated and refined in this initial design. We have demonstrated efficacy of our model by testing on 3D-printed models of the trachea. We aim to conduct further testing on animal models and human cadavers to assess overall procedure time, ventilation, and incidence of misplacement. Upon successful execution, such a design will not only minimize patient complications, but also procedure costs and operating burden on the physicians, making the procedure more accessible and improving patient outcomes.

# Improved Performance of N95 Isolation Masks: Enhancing Communication, Fit, and Comfort

Team Members: Nicole Cavett<sup>1</sup>, Athenia Jones<sup>1</sup>, Julian Kopelove<sup>1</sup>, Kailey Mihavetz<sup>1</sup>, Priscilla Seah<sup>1</sup>  
 Advisors: Dr. William Bentley<sup>1</sup>, Dr. Jeffrey Hasday<sup>2</sup>

<sup>1</sup> The Fischell Department of Bioengineering, University of Maryland, College Park, <sup>2</sup> University of Maryland School of Medicine

## Motivations

N95 respirators are important components to personal protective equipment (PPE) as they are designed to reduce the wearer's risk of inhaling hazardous airborne particles.<sup>1</sup>

Studies show that healthcare workers (HCWs) are poorly compliant with respiratory protection guidelines, especially when a N95 respirator is recommended.<sup>1</sup> It has been reported that users have difficulty breathing, difficulty communicating effectively with patients, and discomfort from humidity and temperature

### Desired N95 Respirator Characteristics

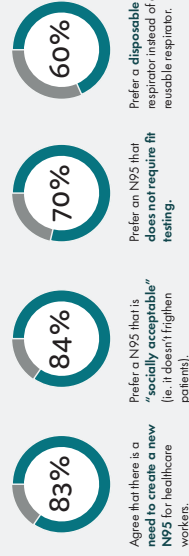


Figure 1 - Desired features in a respirator as report by healthcare workers.<sup>1</sup>

## Design Concepts

To improve compliance and to reduce the risk of disease transmission, we have developed a prototype with features that improve the fit and comfort of the mask.

Our prototype achieves the following design objectives through the incorporation of novel features:

- 1 Improve the fit of the N95 to ensure effective filtration
- 2 Improve ease of communication
- 3 Improve heat and humidity regulation

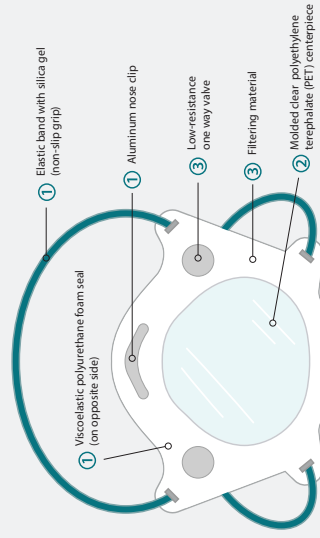


Figure 2 - 2D prototype design concept. Numbers in figure correspond to the design objective.

## Methods

### Temperature and Humidity Testing:

- **Exercise Performed:** Brisk walk for 10 mins. while wearing control (3M 1860) and repeated for prototype
- **Measurement:** Temperature and humidity measurements using a wireless hygrometer (iButton Hydrochron Temperature/Humidity Sensor, MaxIm Integrated)

### Qualitative Comfort and Communication Testing:

- **Exercise Performed:** User performs 25 jumping-jacks, then blind tested (either with control or prototype).
- **Measurement:** Survey using a 5-point likert scale of 1 to 5 (where 1 = least comfortable/ effective, 3 = neutral, 10 = most comfortable, most effective).

### Participants were asked the following survey questions:

- 1 How comfortable is the face seal?
- 2 How comfortable is the temperature of the mask?
- 3 How strong is the smell of the perfume? (1 = cannot smell, 5 = very strong smell)
- 4 When the tester is wearing the mask, how well can you read the tester's lips?



Figure 3. Setup of wireless hygrometer (iButton) in control N95 mask (a) and in the prototype (c) and (d). Fig. 3 (a) and (c) depict the front of the mask.

## Results

Initial testing shows perceived temperature of the prototype is higher due to humidity. Comfort of the seal decreases over time due to high contact pressure. In addition, the transparent window starts off clear but gradually fogs over time. For additional data and biological replicates see hand out provided.

Hygrometer data shows that the prototype significantly reduced temperature within the mask from 33.18(°C) to 31.18(°C) and significantly increased humidity within the mask from 82.31% to 86.12%.

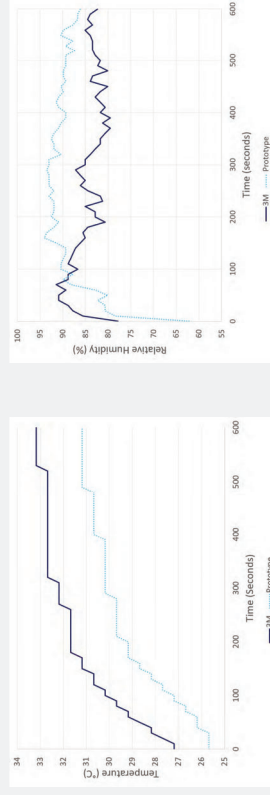


Figure 4. Temperature readings for respirator dead space. Unpaired, two sample t-test used to analyze results between both.

Figure 5. Relative humidity readings for respirator dead space. Unpaired, two sample t-test used to analyze results between both.

Qualitatively, the memory foam seal made the prototype more comfortable around the edges, while also securing a better seal. The perceived temperature was noticeable by the users in both designs. Fogging of the prototype occurred after 4 minutes of active use.

## Novel Filter Media

### Three effective layers:

- 1 Surgical Mask: 99% 0.5 micron particles
- 2 Cellulose fibers: 10% 0.5 micron particles
- 3 Surgical Mask: 99% 0.5 micron particles

Assumed fully aligned pore diameters for the most conservative estimate, the additive layers of the prototype should theoretically filter 99.991% of 0.5 micron particles (vs. 95.000% of 0.3 micron particles in typical N95 mask).<sup>2</sup>

## Conclusions

While maintaining filtration efficiency, our prototype incorporates novel features to improve communication, fit, and comfort from a typical N95 mask.

Design Concept	Typical N95	Prototype
Communication	Completely opaque	Clear PET centerpiece
Comfort	No exhalation valves Charged filter media Thin nose foam pad	2 one-way exhalation valves Charged filter media Viscoelastic polyurethane seal (periphery of mask)

Table 1. Comparison of features between a typical N95 mask (3M 1860) and our prototype.

### Ethical Implications

- Improved comfort will increase compliance, leading to greater personal protection and decreased pathogen transmission.
- Improved communication will help mitigate patient intimidation and anxiety, enabling suffering individuals to seek medical attention.
- Our prototype is universally designed so that the increased visibility of the user's mouth will be assistive to patients who are elderly or who have audio impairments (for lip reading).

## Future Works

Future iterations of the prototype:

- 1 Will incorporate desiccant to decrease humidity
- 2 Will improve fit of the mask to greater variety head forms
- 3 Increase the distance of the prototype to the face to increase

## References

1. Bagg, A. S., Knapp, C., Egan, A. E., & Radonovich, L. J. (2010). Health care workers views about respirator use and features that should be included in the next generation of respirators. *American Journal of Infection Control*, 38(1), 18-25. doi:10.1016/j.ajic.2009.09.005
2. Swaminath, H., Sudhakar, L., Wang, Y., & Zhang, W. (2017). A Disposable Multi-Functional Air Filter. *Paper Towel/Protein Nanofibers with Gradient Porous Structure for Capturing Pollutants of Broad Species and Sizes*. ACS Sustainable Chemistry & Engineering, 5(7), 6293-6301. doi:10.1021/acscchemeng.7b01160

## **Improved Performance of N95 Isolation Masks: Enhancing Communication, Fit, and Comfort**

Nicole Cavett, Athenia Jones, Julian Kopelove, Kailey Mihavetz, Priscilla Seah

Numerous studies show that healthcare workers are poorly compliant with respiratory protection guidelines, especially when a N95 respirator is recommended. Many features of the current N95 masks may contribute to the lack of compliance: temperature and humidity accumulation in the mask as well as pressure from the nose clip and elastic straps may cause discomfort when the N95 is worn for prolonged periods of time. To improve compliance and to reduce the risk of disease transmission, we have developed a prototype with features that improve the fit and comfort of the mask. One-way exhalation valves and novel filter media were used to reduce the temperature and humidity accumulation. Viscoelastic polyurethane foam was used to not only generate a better seal between the mask and the user's face, but also to reduce contact pressure. To facilitate communication, we have we have incorporated a clear polyethylene terephthalate (PET) centerpiece, which permits lip reading and facial expressions to be seen. Preliminary data suggests the prototype increases humidity within the mask while decreasing temperature. Future work includes improving the fit of the mask to greater variety head forms. In addition, we plan to continue development and testing of the filter media, while also testing effectiveness of a desiccant. Ultimately, we hope to accomplish the intended social impact of improving compliance and reduce the risk of disease transmission.

# Detection of Brain-to-Brain Synchrony for Improved Psychotherapy

Faculty & Capstone Advisor: Professor Yang Tao, Fischeil Department of Bioengineering, University of Maryland  
 Michael Dib, Akash Gami, Idrisa Rahman, and Leah Ross  
 Clinical Mentor: Dr. Zhi-De Deng, National Institute of Mental Health, NIH  
 Clinical Mentor: Dr. Marc Lener, Psychiatrist, Chief Executive Officer, Singula Institute



## Motivation

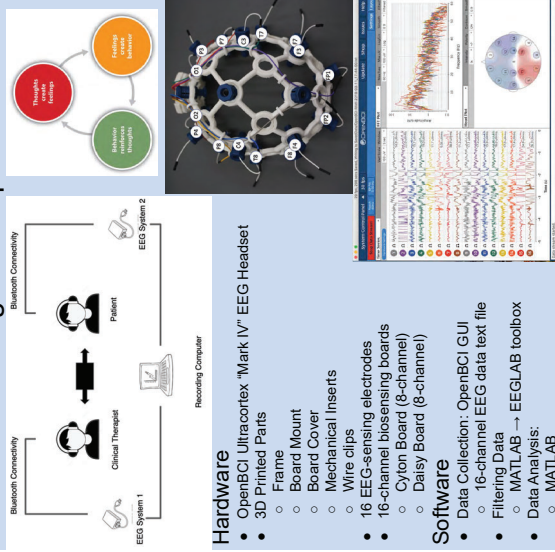
Current methods to treat mental disorders involve cognitive behavioral therapy (CBT). However, CBT provides no method to determine or measure the therapeutic alliance between the clinician and patient. The therapeutic alliance develops as a result of interpersonal synchrony, which is defined as inter-brain coupling.

Currently, the most advanced technology for standard protocol during clinician-patient interaction is simply a voice recorder. Devices and methods involving EEG are used almost exclusively for scientific research. The implementation of EEG into psychiatry and other mental health-related fields has limitless potential in improving the efficacy of clinician-patient interactions. Using and analyzing EEG data from therapy sessions would provide the therapist more insight as to the best treatment method for the patient.

## Objective

- The device will detect EEG signals between a patient and clinician and utilize hyperscanning to determine signal coherence of neural activity to detect spatial and temporal brain-to-brain synchrony.
- The device will display signal coherence results on a recording computer to allow the clinician to adjust their therapy.
- The device will archive the recorded data to serve as a reference to measure the effectiveness of therapy sessions.

## Design Concept



## Testing and Results

$$PLV_{j,k,t} = \frac{1}{N-1} \sum_{i=1}^{N-1} e^{i\phi_j(f,t) - \phi_k(f,t)}$$

Phase Locking Value

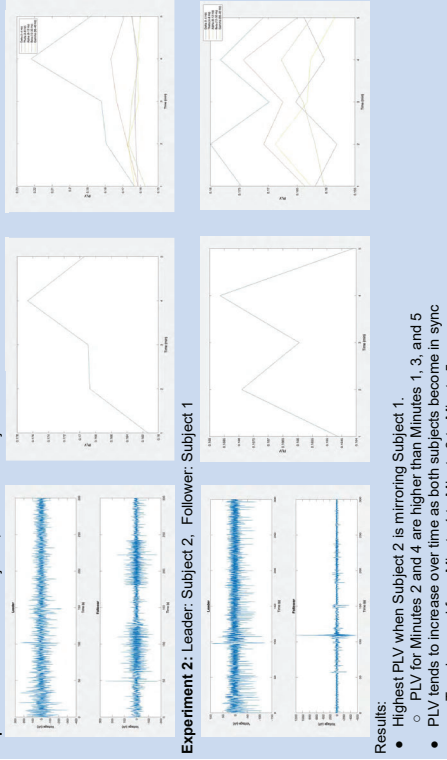
- At a given time and frequency, calculates the absolute value of the sum of the phase difference ( $\phi$ ) differences of two electrodes (j, k) from two individuals of a dyad across N epochs

### Synchrony Task:

Two persons keep each of their index fingers pointed outwards at the index fingers of the other in a face-to-face setting. There is a leader (Subject 1) and a follower (Subject 2).  
**Minute 1:** Subject 1 moves his or her index finger within a 20cm by 20cm square. Subject 2 watches and keeps his or her eyes fixed on the movements of the leader.  
**Minute 2:** Subject 1 continues to move his or her index finger within a 20cm by 20cm square. Subject 2 mirrors the movements of Subject 1.  
 Minutes 3 and 5 are performed as Minute 1. Minute 4 is performed as Minute 2.

### Data Analysis:

- EEGLAB:**
- Select Data to be Sampled
    - Define time frame and/or remove time
    - Reduce Noise and Artifacts of EEG Signal
      - 0.5 to 60 Hz
  - Define channel brain locations
  - Run Independent Component Analysis (ICA)
  - Verify real EEG data, reject fake EEG database
    - 5 frequency bands
      - Delta: 1-4 Hz
      - Theta: 4-8 Hz
      - Alpha: 8-12 Hz
      - Beta: 12-30 Hz
      - Gamma: 30-40 Hz
    - 2 second windows
  - Average interbrain PLV each frequency band
- Experiment 1:** Leader, Subject 1, Follower, Subject 2
- Experiment 2:** Leader, Subject 2, Follower, Subject 1



### Results:

- Highest PLV when Subject 2 is mirroring Subject 1.
- PLV for Minutes 2 and 4 are higher than Minutes 1, 3, and 5
- PLV tends to increase over time as both subjects become in sync
  - Trend upward from Minute 1 to Minute 3 to Minute 5

## Conclusions and Implications

- Phase locking value increases after interaction, showing that over many psychotherapy sessions, synchrony between patient and clinician should increase
- Increased synchrony helps to develop and improve therapeutic alliance, thus improving efficacy of psychotherapy treatments over time
- Potential for further use to understand underlying neural networks involved in cognition, emotion processing, and human interaction
- Potential for this device to be used as a tool for standard of care for psychotherapy patients
- Allows clinicians to deeply understand emotional and behavioral triggers to develop more effective treatment methods
- Potential for debunking stereotypes surrounding mental illness by providing quantitative data supporting CBT
- Moves beyond single brain analysis to study collective brain processes between two individuals

Potential for use in other applications:

- Relationship counseling
- Speed dating
- Group decision making

Ethical Implications:

- Expectation gap: BCI devices are expected to be more effective
- BCI technology is still limited by noise, movement, etc., lots of potential for growth

## Future Works

- Emotional Video
  - Extend the research into evaluating brain synchrony between two subjects watching an emotional video.
- Automatic Data Analysis
  - Develop a Matlab program which will allow for automatic data analysis.
  - Two Click Approach - Therapist selects 2 data files and PLV value is displayed
- Real time feedback analysis
  - Immediate adjustment of psychotherapeutic procedure with the guide of a qualitative display for clinical progress.
  - Current limitations
    - Available technology
    - Processing/Computational speeds (MATLAB ICA)
- Multimodal Signal Analysis
  - Incorporate other phenotypic and physiological analysis modes to collect data such as EMG, EKG, voice analysis or facial learning to give more information on other dynamic detections of coherence.
- EEG headset remodeling
  - Improve comfort level of EEG headset to reflect a more natural conversation.

## References

- Gaetano, B.A. (2005). Cognitive-behavioral therapies: Achievements and Challenges. *Evidence-Based Mental Health, 11*(1), 5.
- Hart, R., Hübner, T., Nurumetova, L., Hanhinen, M., & Pulkkinen, L. (2013). Synchrony of brain and bodies during implicit interpersonal interaction. *Trends in Cognitive Sciences, 17*(3), 10-16. doi:10.1016/j.tics.2013.01.003
- Rasson, U., Ghahramani, A., Ghahramani, B., Garrod, S., and Keysers, C. (2011). Inter-brain coupling: a mechanism for shared understanding. *Philosophical Transactions of the Royal Society B, 366*, 114-121.
- Lachaux, J.P., Rodriguez, E., Martinerie, J., Varela, F.J. (1999). Measuring phase synchrony in brain signals. *Human Brain Mapping, 8*, 194-208.
- Mu, Y., Han, S., & Geland, M.J. (2017). The role of gamma interbrain synchrony in social coordination when humans face territorial threats. *Social cognitive and affective neuroscience, 12*(10), 1644-1653.
- Perkins, T., Lener, M., & G. (2018). Understanding the Direct Induction of Affect as a Component of Cognitive Behavioral Therapy. *Behavioral Sciences, 8*(3), 29.

## **Detection of Brain-to-Brain Synchrony for Improved Psychotherapy**

Michael Dib, Akash Gami, Idrisa Rahman, and Leah Ross

Current models to treat mental disorders mainly include cognitive behavioral therapy (CBT), however, a main limitation of CBT is that it has no way to determine or measure the therapeutic alliance between the clinician and the patient. Previous studies have shown that for two people interacting with each other, there is a neural association that develops between them. This idea can have great implications in the field of psychotherapy. The detection of brain synchrony between a patient and a therapist can show how engaged they are with each other during a therapy session. Although psychotherapy is an established field and treatment for mental disorder alleviation, technologies that allow the accurate detection of a large array of biologically generated signals are relatively new and constantly being renovated. The most advanced technology used currently for standard protocol during clinician-patient interaction in therapy sessions is simply a voice recorder. Devices and methods such as electroencephalography (EEG), facial pattern recognition, and electrodermal detection are used almost exclusively for scientific research. The implementation of these methods into psychiatry and other mental health-related fields has limitless potential in improving the efficacy of clinician-patient interactions. While it would traditionally take several sessions for a clinician to understand the individual needs of a new patient and to decide the most appropriate methods of therapy, using these technologies would give the clinician a far greater idea of how to approach the patient even by the second session. The product we developed aims to capitalize upon the concepts of social interaction and hyperscanning to be able to detect and measure the therapeutic alliance between the clinician and the patient by detecting brain to brain synchrony signals via EEG. This provides the greatest ecological validity due to its non-invasiveness and its ability to be used in a typical social face-to-face therapist-patient interaction.